ACS OMEGA

Open Access

http://pubs.acs.org/journal/acsodf

Article

Novel 2D Layered MXene Nanofluids for Enhancing the Convective Heat Transfer Performance of Double-Pipe Heat Exchangers

Kodi Rajesh Kumar and Aabid Hussain Shaik*

Cite This: *ACS Omega* 2024, 9, 41758−41775

Read Online

ACCESS | Metrics & More | Article Recommendations | Supporting Information

ABSTRACT: This paper proposes a new class of novel 2D layered structured materials, such as MXene (MX), for the synthesis of innovative nanofluids as coolants to evaluate the convective heat transfer performance of a double-pipe heat exchanger (DPHE). Convective heat transfer experiments were successfully conducted in lab-scale fabricated DPHE using low-concentration MXene nanofluids by varying the volume concentration of MXene nanoparticles (0.01−0.05 vol %) in different base fluids. The influence of the MXene nanofluids on various convective heat transfer parameters, such as LMTD, Nusselt number, heat transfer coefficient, and heat transfer rate without using any inserts in the DPHE was experimentally investigated. The results of the experiments revealed that the heat transfer coefficient and Nusselt number increase with increasing Reynolds number (Re) and concentration of MXene nanoparticles in the base fluids. Maximum enhancement in heat transfer coefficient (126%) was achieved for methanol-based MXene nanofluids at 0.05 vol %. Moreover, the Nusselt number exhibits a maximum enhancement of ∼50% for methanol- and water-based MXene nanofluids. In contrast, the thermal performance factor was also estimated, and it was observed that water- and methanol- based MXene nanofluids showed higher values than castor oil- and silicone oil-based MXene nanofluids. Finally, the LMTD and heat transfer coefficients were successfully validated using Aspen HYSYS 12.1 software.

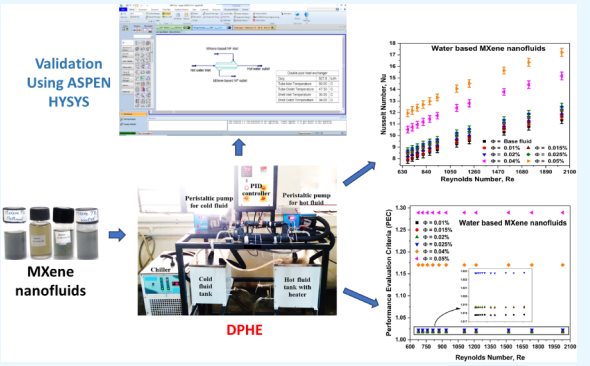

1. INTRODUCTION

Convective heat transfer is an essential technique for enhancing energy efficiency and is widely used in many industries, including the chemical, aircraft, energy, and power motor industries.[1,2] This process is crucial for efficient heat exchange, temperature regulation, and affects various applications.[3] Improving the heat transfer efficiency is crucial for thermal systems.[4] The double pipe unit, which consists of two concentric pipes with opposing hot and cold fluid flows, is one of the simple and most commonly used and basic types of heat exchangers for improving heat transfer efficiency.[5,6] Heat exchangers are used in air conditioning, refrigeration, space applications, electronics, food, chemical processing, and power generation industries.[6] The efficiency and heat transfer rate of exchangers are affected by the fluid characteristics, flow regime, geometry, and operating conditions.[7]

Twisted tapes,[1,8] fins,[9] baffles,[10] corrugated tubes,[11] and butterfly inserts[12] are a few types of the approaches that have been suggested to improve heat transfer performance by passive techniques.[4,13] On the other hand, employing a power source to create surface and fluid vibrations by introducing electrohydrodynamic systems is part of the active heat transfer approach.[14] In most cases, passive techniques yielded superior outcomes than active ones. In contrast, introducing nanoparticles into a passive technique enhances the rate of heat transmission[4,15] and Table 1 summarizes various research findings on heat transfer investigations using nanofluids.

According to Mukherjee et al.[21] and Choi,[22] nanofluids are currently the most practical choice for a cooling media. They are generated by dispersing nanoparticles, mostly metals or metal oxides, which typically range in size from 1 to 100 nm, into base fluids and referred to as "nanofluids", and they have a significantly higher thermal conductivity than convectional fluids. Loading nanoparticles into base fluids is expected to increase thermal conductivity, which may lead to improved heat transfer capabilities.[23] Dong et al.[1] reported that water-EG-based silicon dioxide nanofluids (6.0 wt.%) boosted the heat transfer coefficient by 36.1% at 25 °C under laminar flow region and also showed strong corrosion resistance. Zakeri and Emami[6] conducted experimental and numerical studies on DPHE using water-based graphene oxide nanofluids and reported significant improvements in the heat transfer coefficient, pressure drop, and friction factor by 85, 111, and

Received: July 1, 2024
Revised: August 24, 2024
Accepted: August 28, 2024
Published: September 23, 2024

Table 1. The Comparative Study on the Performance of Heat Exchangers Using Different Nanofluids

						Percentage enhancement (%)				
Reference	Base fluid	Nanoparticles	Concentration (vol.% and wt.%)	Type of insert	Flow type	*Nu*	*h*	Δ*P*	*f*	*U*
[12]	Water	TiO_2	0.1−0.3	Butterfly inserts	Laminar	40	-	-	60	-
[13]	Water	SiO2	0−4	No	Turbulent	32	9	29	17	-
[15]	Water	Fe_3O_4	0.005−0.06	No	Turbulent	14	19	-	10	-
[16]	Ionanofluid	MXene	0.01−0.1	Twisted tape	Laminar	136	-	-	27	-
[17]	Water	Fe_3O_4	0.005−0.06	Longitudinal strip inserts	Turbulent	41	30	-	12	-
[18]	Water	WO_3	0.5−3.0	Twisted tape, ribs	Turbulent	18	-	22	-	14
[19]	Water	TiO_2	2.0−3.0	-	Both Laminar and turbulent	14	-	-	-	60
[20]	Water	γ-Al_2O_3	0.25−1.0	-	Turbulent	10	60	85	10	-

72%, respectively, for the 0.1 vol% concentration of nanoparticles compared to other nanofluids prepared using nanoparticles of silver, Al_2O_3, and TiO_2. In another study by Duangthongsuk and Wongwises,[5] the convective heat transfer coefficient was increased by 11% for a water-based titanium oxide nanofluid at 0.2 vol.% concentration of nanoparticles. Jayranaiwachira et al.[24] investigated the thermal hydraulic performance and entropy of a uniform heat flux tube with louvered corner-curved baffle tape, and their outcomes revealed that the friction factor (f) and Nusselt number (Nu) were enhanced by 19.2 and 4.4 times, respectively, compared with the results obtained using a plain tube. Wu et al. (2024) enhanced the heat transfer performance in a tube using a multi-V-winglets vortex generator and reported 130.57−156.42% increase in Nu followed by a decrease in the friction factor by creating punched holes on the surface of the generator.[25] Similarly, Louahdi et al. (2024) stated that the thermohydrodynamic performance of a heat exchanger was improved using perforated semicircular inserts in the heat exchanger and also confirmed that the perforations in the insets stimulate the uniformity in the fluid flow, thereby reducing pressure losses.[26] Kavitha et al.[27] investigated DPHE using CuO nanofluids with volumetric concentrations ranging from 0.002 to 0.004% and concluded that h_{avg} was enhanced. Titanium oxide water-based nanofluids synthesized by Khedkar et al.[19] showed a 14% increase in heat transfer coefficient when a double-pipe heat exchanger is loaded with at 3 vol.% concentrated nanofluid. Darzi et al.[20] evaluated the impact of an Al_2O_3/water nanofluid at volume concentrations of 0.25−1% on a DPHE and found that nanoparticles improved the heat exchanger functionality without noticeably increasing the pressure drop under turbulent flow conditions.

Nanofluids research has gained new dimensions with the introduction of extraordinarily conductive nonmetallic nanoparticles, including graphitic, carbon nanotubes (CNT), and graphene nanoparticles.[16,28] In 2011, MXenes as a novel material developed by Yury Gogotsi and Michel Barsoum at Drexel University in the United States,[29−31] instantly sparked the interest of multiple researchers due to its layered structure,[32,33] hydrophilic nature,[34] lack of toxicity,[31] and excellent thermal and electrical conductivity,[35,36] and it is currently proving to be an important concern in several kinds of engineering fields.[37]

MXene is produced from three-dimensional (3D) MAX phases by selectively etching the "A" layer, which is positioned in 14 and 13 groups in the p-block elements.[16,29,30,36] The usual formula is $M_{n+1}X_nT_x$ (n = 1, 2, and 3). T_x denotes the surface termination (such as F, O, and OH), M refers to the early transition metal, and X denotes either elements of carbon or nitrogen.[29,30] MXenes are now doped in base fluid to form MXene-based nanofluids and promising energy- storage substances because they are multilayer, highly electrically conductive materials.[38,39] The preparation procedure, which also controls the crystallinity and shape of the material, affects the performance of MXenes in various applications.[40] According to Sajid and Ali,[28] the connections between the MXene layers are more powerful than the van der Waals interactions and are not damaged by mechanical or shearing forces. Rubbi et al.[41] studied hybrid PV/T solar systems using Ti_3C_2/soybean oil as the coolant and reported an 84.25% increase in thermal efficiency at a mass flow rate of 0.07 kg/s for a 0.125 wt.% concentrated nanofluid with a reduction in the surface temperature by 14 °C. According to studies carried out by Aslfattahi et al.[42] the viscosity of MXene/silicone oil nanofluids increased with loading but remained almost constant and observed a reduction in viscosity by 32%, followed by a 64% enhancement in thermal conductivity for the 0.1 wt.% concentrated nanofluid. Similarly, Samylingam et al.[43] evaluated the performance of palm oil-based MXene nanofluids in a PV/T system with concentrations ranging from 0.01−0.2 wt.% and found that the system heat dissipation, electrical efficiency, and thermal efficiency increased by 8.5%, 13.8%, and 11.2%, respectively, compared with water-based aluminum oxide (Al_2O_3) nanofluids at 0.07 kg/s mass flow rate.

From the overview of the literature, it can be clearly observed that most of the works were conducted on increasing the thermal performance of the heat exchangers using twisted tapes in its geometry and by circulating metal/metal oxide-based nanofluids with high concentrations of nanoparticles in the base fluids as a coolant. Moreover, relatively limited research has been conducted on utilizing two-dimensional layered structures, primarily composed of MXenes at very low concentrations, for performing convective heat transfer studies in basic heat exchangers, such as DPHE. Hence, we propose a novel layered 2D material such as MXenes to prepare water, methanol, silicone oil, and castor oil-based MXene nanofluids at very low concentrations (less than 0.05 vol %) to evaluate and enhance the heat transfer performance in a double-pipe heat exchanger without utilizing any inserts/twisted tapes under laminar flow region. This work also focuses on comparing the experimental heat transfer performance with the performance obtained by using the ASPEN HYSYS simulation software.

https://doi.org/10.1021/acsomega.4c06080
ACS Omega 2024, 9, 41758−41775

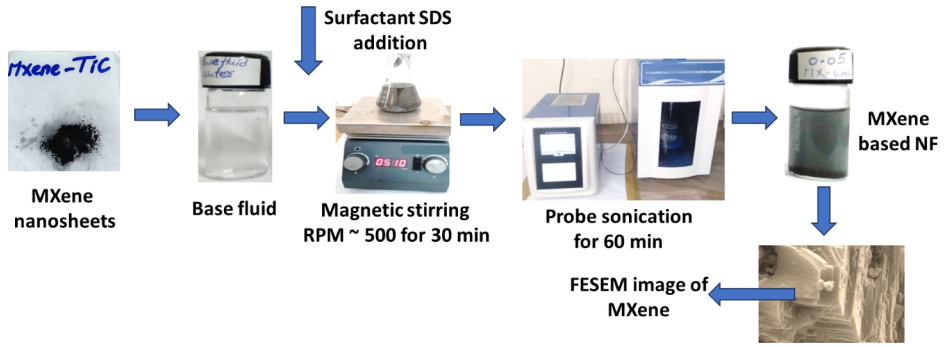

Figure 1. Synthesis of MXene nanofluid by two-step method.

Table 2. Thermophysical Properties of Water-Based MXene Nanofluids at 30 °C

Φ (vol %)	k (W/m. K)	ρ (kg/m^3)	C_p (J/kg K)	μ (pa.s)	Pr
0	0.598	995.65	4178	0.0007972	5.572401
0.01	0.606	995.74	4036.69	0.000842	5.608734
0.015	0.614	996.1	3967.87	0.000871	5.628689
0.02	0.636	996.38	3901.14	0.000942	5.778104
0.025	0.655	996.57	3836.4	0.000991	5.804385
0.04	0.688	996.95	3653.28	0.00119	6.3189
0.05	0.692	997.14	3539.69	0.00129	6.598555

Table 3. Thermophysical Properties of Methanol-Based MXene nanofluids at 30 °C

Φ (vol %)	k (W/m. K)	ρ (kg/m^3)	C_p (J/kg K)	μ (pa.s)	Pr
0	0.202	778.1	2560	0.000507	6.425347
0.01	0.214	779.35	2404.55	0.000573	6.438351
0.015	0.231	779.57	2359.78	0.000633	6.46641
0.02	0.25	779.85	2316.83	0.000699	6.477857
0.025	0.265	780.24	2275.59	0.000779	6.664228
0.04	0.27	783.19	2161.13	0.000859	6.875595
0.05	0.304	785.66	2091.72	0.001005	6.915061

Table 4. Thermophysical Properties of Castor Oil-Based MXene Nanofluids at 30 °C

Φ (vol %)	k (W/m. K)	ρ (kg/m^3)	C_p (J/kg K)	μ (pa.s)	Pr
0	0.177	939.38	1900	0.34500	3703.39
0.01	0.179	940.64	1846.21	0.35200	3630.586
0.015	0.183	941.43	1820.65	0.35559	3537.708
0.02	0.193	943.43	1795.82	0.35923	3342.508
0.025	0.209	945.03	1772	0.36292	3076.999
0.04	0.223	949.06	1704.57	0.37435	2861.453
0.05	0.234	954.2	1662.95	0.38227	2716.66

Table 5. Thermophysical Properties of Silicone Oil-Based MXene Nanofluids at 30 °C

Φ (vol %)	k (W/m. K)	ρ (kg/m^3)	C_p (J/kg K)	μ (pa.s)	Pr
0	0.151	946.48	1200	0.2211	1757.086
0.01	0.152	947.72	1157.42	0.22559	1717.773
0.015	0.154	948.79	1146.69	0.22789	1696.843
0.02	0.155	952.49	1136.3	0.23022	1687.71
0.025	0.157	952.65	1126.25	0.23258	1668.456
0.04	0.162	952.81	1097.94	0.23991	1625.96
0.05	0.166	956.58	1080.47	0.24499	1594.579

2. EXPERIMENTAL STUDY

2.1. Synthesis of MXene-Based Nanofluids and Thermophysical Properties. MXene nanosheets were synthesized by following the method published in our previous article.[44] A two- step method was used to synthesize MXene-based nanofluids. The synthesized MXene Titanium carbide (TiC) nanosheets were weighed according to their volume concentrations ranging from 0.01 to 0.05% and then dispersed separately into different types of base fluids, like methanol, water, silicone oil, and castor oil, containing sodium dodecyl sulfate (SDS) surfactant using a probe-type ultrasonicator. The

https://doi.org/10.1021/acsomega.4c06080
ACS Omega 2024, 9, 41758−41775

Table 6. The Details of DPHE

Material of construction	Thermal conductivity (W/m. K)	Length of the exchanger	Inner pipe		Outer pipe	
			Inner diameter (ID) (D_i)	Outer diameter (OD) (D_{io})	Inner diameter (D_o)	Outer diameter (D_{oo})
Stainless steel	45	0.3 m	0.008 m	0.01 m	0.016 m	0.021 m

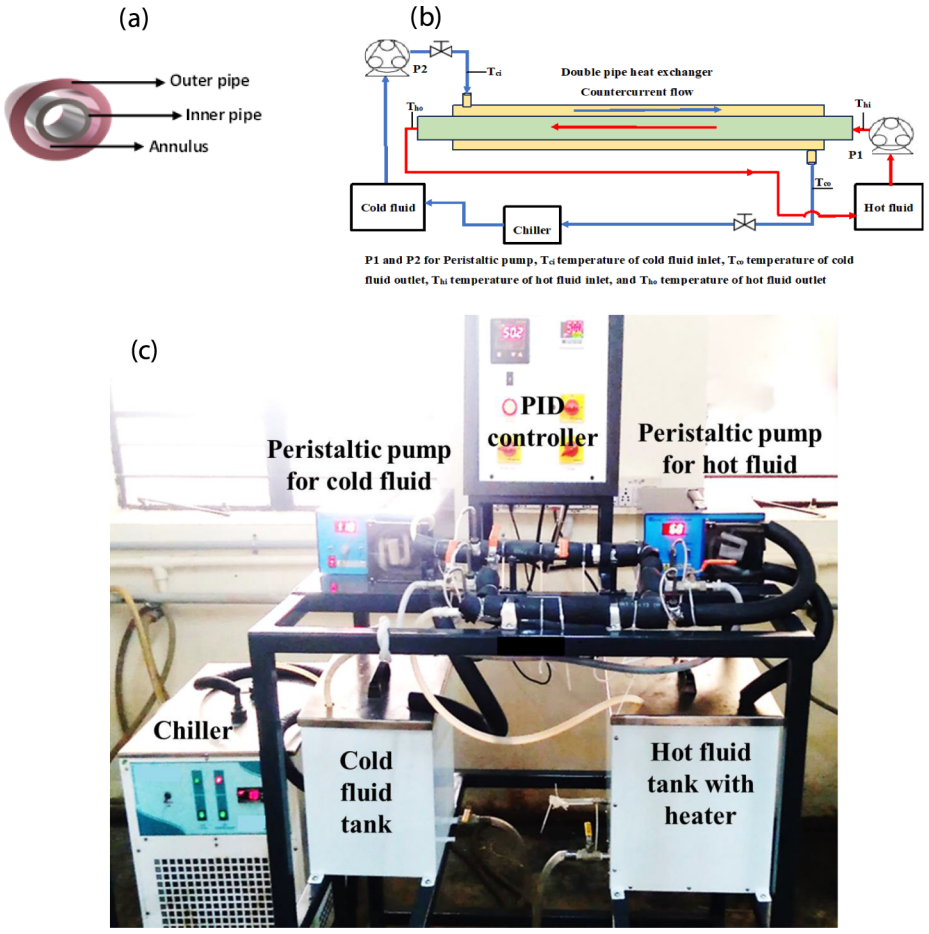

Figure 2. (a) Cross-section of the heat exchanger; (b) schematic showing the counter flow pattern; and (c) front view of experimental DPHE.

main objective of our work was to enhance the convective heat transfer performance of DPHE using a low-concentration of MXene nanoparticles. This was the research gap that we identified from the literature. Most of the literature focused on increasing the performance of heat exchangers using high concentrations of nanoparticles (more than 0.1 vol.% concentration). Due to this reason, we decided to keep the concentration of MXene nanoparticles as low as possible (0.01−0.05 vol %) to achieve the maximum heat transfer performance. The detailed procedure is illustrated in Figure 1.

The key parameters for assessing the heat transfer merits of nanofluids are their thermophysical properties, such as thermal conductivity, specific heat capacity, viscosity, and density. These properties were studied and collected from our previously published article,[42] as shown in Tables 2− 5, respectively.

2.2. Experimental Setup. A modular simple DPHE was fabricated at the lab scale by considering cost factors and also conducting the convective heat transfer studies using MXene nanofluids. Stainless steel material was chosen for tube selection due to its good corrosion resistance. Since we wanted to increase the convective heat transfer performance without using baffles/twisted tapes, we selected a very concise and straight horizontal concentric pipe (without baffles/twisted tapes) with a length of 300 mm, inner diameter of the inside tube of 8 mm with a thickness 1 mm, and outer pipe of 16 mm inner diameter and a thickness of 2.5 mm. The outer pipe is twice the size of the inner pipe to accommodate a greater volume of nanofluids. The detailed configuration of the fabricated DPHE is shown in Table 6. The heat exchanger has two concentric tubes in which the nanofluids as cold fluid (coolant) circulate in the outer pipe and distilled water is circulated as hot fluid in the inner tube under countercurrent flow arrangement, as shown in Figure 2a,b. DPHE is well insulated to prevent any heat losses. Exactly, five thermocouples were installed, four of which were used to determine the inlet and outlet temperatures of hot and cold fluid from DPHE, and another one was placed in the hot fluid tank to measure the temperature of the hot fluid in the tank. In addition, two peristaltic pumps were employed to circulate and control the flow rates of the cold and hot fluids. The temperature of the hot fluid was consistently maintained at 50 °C, and the temperature of the cold fluid was steadily maintained at 30 °C with the help of a chiller.

https://doi.org/10.1021/acsomega.4c06080
ACS Omega 2024, 9, 41758−41775

Figure 2c illustrates the experimental setup of the fabricated DPHE from a front view. Briefly, it has four main crucial sections, such as heating, cooling, chilling, and a proportional-integral-derivative (PID) controller with an indicator. The hot fluid storage tank was made up of 1 in. thick stainless-steel to prevent heat losses to the surroundings, and it consisted of a 1500 W electrical immersion heater and a drain valve for draining the fluid. The temperature of the fluid is controlled and maintained constantly using the PID, and a peristaltic pump was used to circulate the hot fluid into the DPHE. Cold fluid, i.e., MXene nanofluids were retained in a small flask surrounded by a cooling jacket. A chiller is used to maintain the temperature of nanofluids (cold side) at around 30 °C by circulating cold water constantly in a jacketed container.

To determine the performance of the heat exchanger, initially pure base fluids such as water, methanol, castor oil, and silicone oil at 30 °C were circulated in the annulus with the help of a peristaltic pump (speed ranging from 20 to 190 rpm), which acts as cold fluids and hot fluids, i.e., distilled water with an input temperature of 50 °C is passed through the inner tube at 1220 Re. Later, the same conditions were used for investigating convective heat transfer using MXene-based nanofluids with varying volumetric concentrations (0.01, 0.015, 0.02, 0.025, 0.04, and 0.05%) respectively.

2.3. Data Reduction for Convective Heat Transfer Studies. The experimental data was used to calculate various convective heat transfer parameters to assess the performance of DPHE using MXene nanofluids. The hydraulic diameter for the annulus (d_{ho}) can be determined by the following expression:[17]

$$d_{ho} = \frac{A \times 4}{P} = D_o - D_i \tag{1}$$

where A is the flow area and determined as $A = \frac{\pi}{4}(D_o^2 - D_i^2)$, P is a wetted perimeter, D_i is the inner tube diameter, and D_o is the outer pipe diameter.

The heat transfer rates for cold and hot fluids are computed by utilizing eqs 2 and 3.

Heat gained by cold or nanofluids (annulus side fluid):

$$Q_c = \dot{m}_c{}^* C_c{}^* (T_{c,o} - T_{c,i}) \tag{2}$$

Heat lost by hot water (tube side fluid):

$$Q_h = \dot{m}_h{}^* C_{ph}{}^* (T_{h,i} - T_{h,o}) \tag{3}$$

The average rate of heat transfer is calculated using the following equation:

$$Q_{\text{avg}} = \frac{(Q_h + Q_c)}{2} \tag{4}$$

where Q represents the heat transfer rate, subscripts c, h, i, and o stand for cold fluid, hot fluid, inlet, and outlet, respectively, $\dot{m}$ is designated as the mass flow rate of fluid, C_p is labeled as specific heat, T_h and T_c are nominated as temperature of hot and cold fluids, respectively.

The logarithmic mean temperature difference (LMTD) under the counter-flow pattern was estimated as follows.

$$\Delta T_{\text{LMTD}} = \frac{(T_{\text{hf},i} - T_{c,o}) - (T_{\text{hf},o} - T_{c,i})}{\ln \frac{(T_{\text{hf},i} - T_{c,o})}{(T_{\text{hf},o} - T_{c,i})}} \tag{5}$$

where $T_{\text{hf,i}}$ and $T_{\text{hf},o}$ temperatures of hot fluid are at the inlet and outlet. Whereas $T_{c,i}$ and $T_{c,o}$ are temperature of cold fluid at the inlet and outlet, respectively.

The average temperatures of cold fluid ($T_{c\ \text{avg}}$) and hot fluid ($T_{\text{hf avg}}$) were calculated by using the following equation

$$T_{c\ \text{avg}} = \frac{(T_{c,i} + T_{c,o})}{2} \quad \text{and} \quad T_{\text{hf avg}} = \frac{(T_{h,i} + T_{h,o})}{2} \tag{6}$$

The overall heat transfer coefficient (U) is computed as follows:

$$U = \left(\frac{Q_{\text{avg}}}{\text{LMTD} \times A} \right) \tag{7}$$

The Reynolds number for nanofluids and the hot fluids is calculated based on the fluid viscosity, density, and flow rates as follows:

$$Re_{\text{nf}} = \left(\frac{D_o{}^* \rho^* v}{\mu} \right)_{\text{nf}} \tag{8a}$$

$$Re_{\text{hf}} = \left(\frac{D_i{}^* \rho^* v}{\mu} \right) \tag{8b}$$

where Re_{nf} and Re_{hf} denotes the Reynolds number of nanofluid (nf) and hot fluid (hf), μ stands for viscosity, and ρ represents density, respectively.

Moreover, the Nusselt number is one of the important dimensionless numbers that affects the heat transfer in working fluids. Since the calculated Re is less than 2300, the Sieder and Tate equation was used to determine the Nusselt number for all fluids.[4] The following Nusselt number equations were applied to the inner and outer pipes of DPHE.

$$Nu_i = 1.86 \times \left(\frac{P_r{}^* D_i{}^* Re_i}{L} \right)^{1/3} \times \left(\frac{\mu_b}{\mu_w} \right)^{0.14} \tag{9a}$$

$$Nu_o = 1.86 \times \left(\frac{P_r{}^* D_o{}^* Re_{nf}}{L} \right)^{1/3} \times \left(\frac{\mu_b}{\mu_w} \right)^{0.14} \tag{9b}$$

Considering the wall temperature, T_{wall},[4] as a starting point, μ_w may be roughly expressed as:

$$T_{\text{wall}} \cong 0.5 \times \left(\left(\frac{T_o + T_i}{2} \right) + \left(\frac{t_i + t_o}{2} \right) \right) \tag{10}$$

where subscript b refers to bulk, T denotes tube side temperature, and t stands for annulus temperature.

The friction factor for laminar flow inside as well as outside the tube was determined using the Darcy friction factor equation, which is represented by eqs 11 and 12.[4]

$$f_i = \frac{64}{Re_i} \tag{11}$$

Equation governing flow via annulus or outer pipe (D_o), is indicated by eq 12

$$f_o = \frac{64}{Re_{\text{nf}}} \times \left(\frac{(k^2 + 1)}{(1 - k)^2} + \frac{(k + 1)}{(1 - k)^* \ln k} \right)^{-1}, \quad \text{where } k = \frac{D_i}{D_o} \tag{12}$$

https://doi.org/10.1021/acsomega.4c06080
ACS Omega 2024, 9, 41758−41775

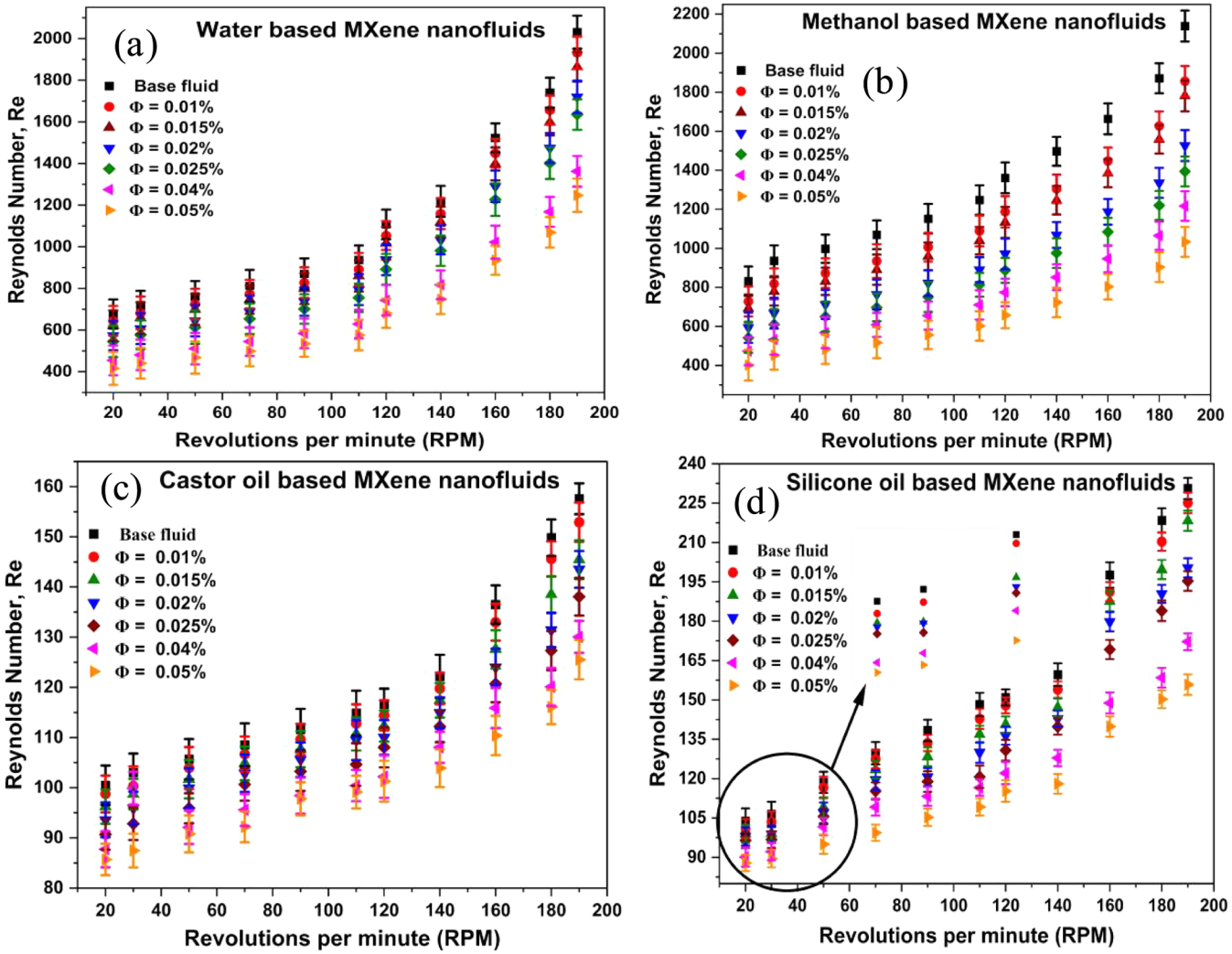

Figure 3. Effect of RPM on the Reynolds number of (a) water-based, (b) methanol-based, (c) castor oil-based, and (d) silicone oil-based MXene nanofluids.

The heat transfer coefficient (ho) under annulus region was determined using the hydraulic diameter (d_{ho}), Nusselt number (N_u), and thermal conductivity (k) values of nanofluids from Table 2 as follows:

$$h_o = \frac{(N_{uo}{}^{*}k_{nf})}{d_{ho}} \tag{13}$$

Based on the viscosity, thermal conductivity, and specific heat of the nanofluids, the Prandtl number (Pr) is computed using the equation below

$$Pr_{nf} = \left(\frac{C_p{}^{*}\mu}{k}\right)_{nf} \tag{14}$$

The pressure drop (ΔP) for hot fluid and nanofluids was calculated using the following equations

$$f_{hf} = \frac{\Delta P_{hf}}{\left(\frac{L}{D_i}\right) \times \left(\frac{v^2 \times \rho_{hf}}{2}\right)} \tag{15a}$$

$$f_{nf} = \frac{\Delta P_{nf}}{\left(\frac{L}{D_o}\right) \times \left(\frac{v^2 \times \rho_{nf}}{2}\right)} \tag{15b}$$

where v is the velocity of the fluid in (m/s).

The following eq 16 was used to evaluate the performance evaluation criteria (PEC) using the frictional losses and the Nusselt number enhancement ratio as follows.[12,16,45,46]

$$\mathrm{PEC} = \frac{\left(\frac{Nu_{nf}}{Nu_{bf}}\right)}{\left(\frac{f_{nf}}{f_{bf}}\right)^{1/3}} \tag{16}$$

where Nu_{nf}, Nu_{nf}, f_{nf}, and f_{bf} are Nusselt number and frictional losses for the nano and base fluids, respectively.

Accuracy is performed in terms of deviation analysis, eq 17 is used to compute the percentage deviation[47,48]

$$\mathrm{Deviation} = \frac{(\mathrm{Predicted} - \mathrm{experimental})}{\mathrm{experimental}} \times 100 \tag{17}$$

3. RESULTS AND DISCUSSIONS

The objective of the current work is to investigate the effects of different operating parameters on the convective heat transfer coefficients (HTC) of four different types of MXene-based nanofluids. Data analysis for these studies was based on steady-state measurements of nanofluids.

https://doi.org/10.1021/acsomega.4c06080
ACS Omega 2024, 9, 41758−41775

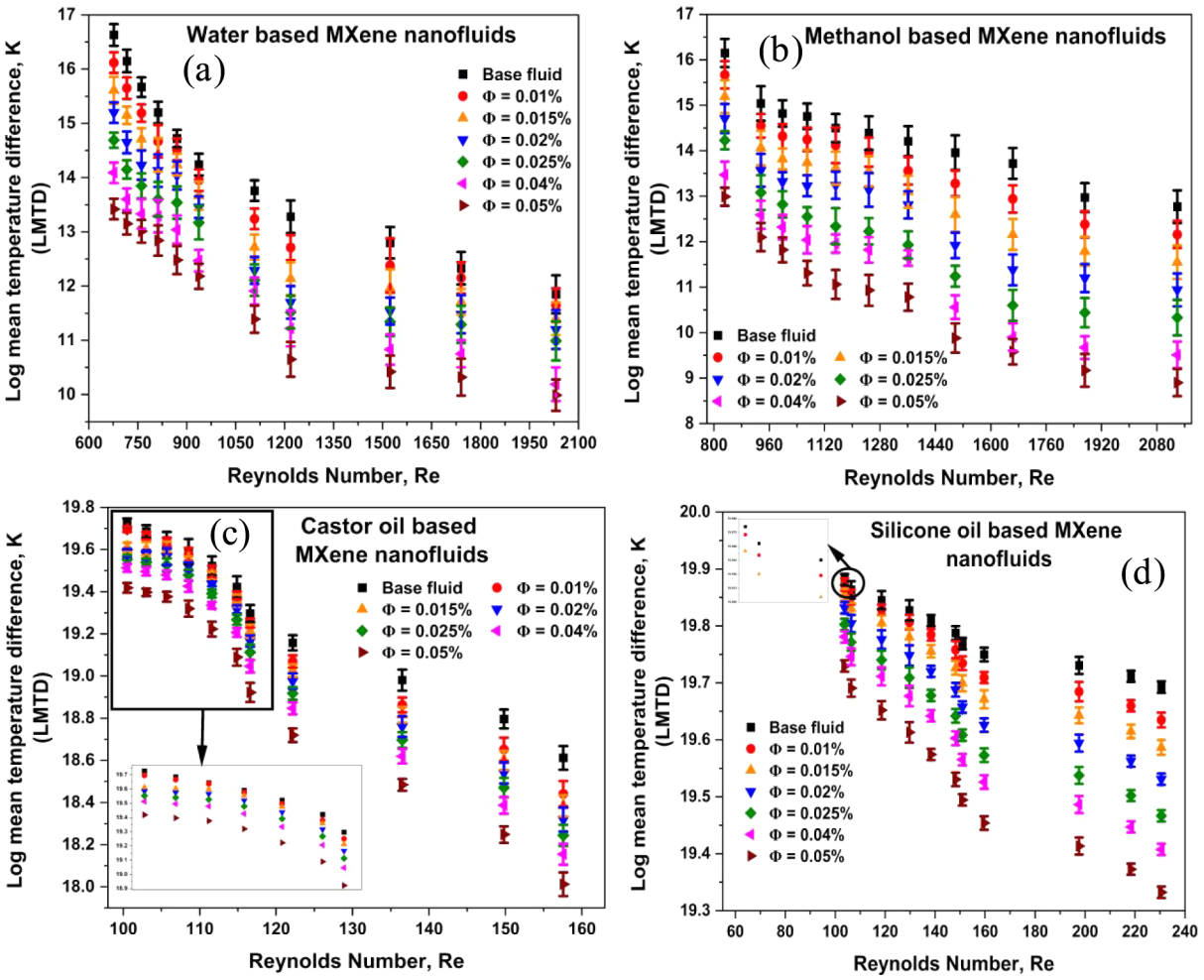

Figure 4. Effect of Re on the LMTD of (a) water-based, (b) methanol-based, (c) castor oil-based, and (d) silicone oil-based MXene nanofluids at various concentrations.

Enhancement of all parameters was calculated using the below eq 18[6]

$$e = \left(\frac{P_{nf} - P_{bf}}{P_{bf}}\right) \times 100 \tag{18}$$

where e is the percentage of enhancement, P represents various parameters, such as Nusselt number, heat transfer coefficient, friction factor, and pressure drop. *nf and bf* represent nanofluid and base fluids, respectively.

3.1. Effect of Revolutions Per Minute (RPM) on Reynolds Number (*Re*). *Re* was computed for both cold and hot streams using the abovementioned eqs 8a and 8b). *Re* of the hot fluid was maintained constant at 1220.25, and *Re* of all the base fluids and MXene nanofluids was computed using the data obtained from Tables 2 and 6, as shown in Figure 3. From Figure 3a− d, it can be observed that the *Re* increases with an increase in the RPM of the pump for all the MXene-based nanofluids, which could be due to an increase in the flow rate. Moreover, methanol-based fluids exhibited a slightly higher increment in *Re* due to their low viscosity anddensity compared to the rest of the fluids (Figure 3b). Likewise, castor oil- and silicone oil-based fluids showed lower *Re* due to their high viscosity values (Figure 3c,d).

3.2. Effect of Reynolds Number on Log Mean Temperature Difference (LMTD) and Validation of Experimental LMTD with LMTD Obtained Using ASPEN HYSYS Software. The heat exchanger's thermal performance was evaluated using the logarithmic mean temperature difference (LMTD) between the two types of fluid (hot and cold streams). The LMTD was calculated experimentally using eq 5 and verified by Aspen HYSYS simulation. Aspen HYSYS 12.1 version with the NRTL thermodynamic fluid package method was used to simulate the LMTD. A representation of the HYSYS simulator is shown in Figure S1. The effect of Reynolds number on the experimental LMTD of all MXene nanofluids are represented in Figure 4 and the validated LMTD using the software along with the percentage variance are reported in Table S1−S4, respectively, for water-based, methanol-based, castor oil-based, and silicone oil-based MXene nanofluids. The average percentage deviation is found from eq 20 and the reported LMTD for the water-based MXene nanofluids was 1.49%, the methanol-based MXene nanofluids was 0.785%, and the silicone oil- and castor oil-based MXene nanofluids were −1.73% and −2.2%, respectively.

Figure 4 shows that LMTD decreases with respect to the increase in Re and concentration of MXene nanoparticles in all of the base fluids. A greater thermal capacity dispersion is indicated by a reduced LMTD value.[45] Compared with base fluids, the MXene-based nanofluids indicated a good percentage decline in LMTD values, as reported in Table 7.

https://doi.org/10.1021/acsomega.4c06080
ACS Omega 2024, 9, 41758−41775

Table 7. Reduction in the LMTD Values Comapred to Base Fluids

	Average % reduction in the LMTD for different nanofluids			
Φ (vol %)	Water-based MXene NF	Methanol-based MXene NF	Castor oil-based MXene NF	Silicone oil-based MXene NF
0.01	2.78	3.91	0.33	0.16
0.015	5.67	7.78	0.57	0.32
0.02	8.09	11.46	0.79	0.51
0.025	10.3	16.38	1.06	0.75
0.04	13.96	20.44	1.38	0.95
0.05	17.06	24.88	2.0	1.29

3.3. Effect of Reynolds Number and Concentration of MXene Nanoparticles on Heat Transfer Rate (*Q*) and Overall Heat Transfer Coefficient (*U*). The hot fluid at 50 °C (323.15 K) continues to circulate on the tube side at constant Reynolds number (1220) and the cold fluid (MXene-based nanofluids) is allowed to flow on the shell side at a constant temperature of 30 °C (303.15 K) with variable flow rates using a peristaltic pump. Figure 5 highlights the variation of Re and nanofluid concentrations with respect to the heat transfer rate (Q). The heat transfer rate is estimated using eqs 2−4). From Figure 5 a−d, it was observed that the rate of heat transfer increased with an increasing Reynolds number and concentration of MXene nanoparticles in all the base fluids, possibly due to the increase in thermal conductivity and an increase in the flow rate.

Subsequently, the overall heat transfer coefficient (U) was also estimated using eq 7 for various MXene-based nanofluids, with respect to the Reynold number and concentration of MXene nanoparticles shown in Figure 6. From Figure 6a−d, it can be seen that the overall heat transfer coefficient increases with respect to the increase in the Reynolds number and concentration of nanoparticles for all the MXene-based nanofluids. This considerable increase in U is due to the decrease in the LMTD, as shown in Figure 4. The enhancement percentage of U is listed in Table 8. Moreover, U was also validated using Aspen HYSYS 12.1 software, and outcomes were reported as Supporting Information Tables S5−S8 for water-based, methanol-based, castor oil-based, and silicone oil-based MXene nanofluids. The percentage deviation by utilizing eq 20 is determined for water-based as −1.24%, methanol-based is around −5.35%, 1.79% for castor oil- based, and silicone oil-based as 2.42%, respectively.

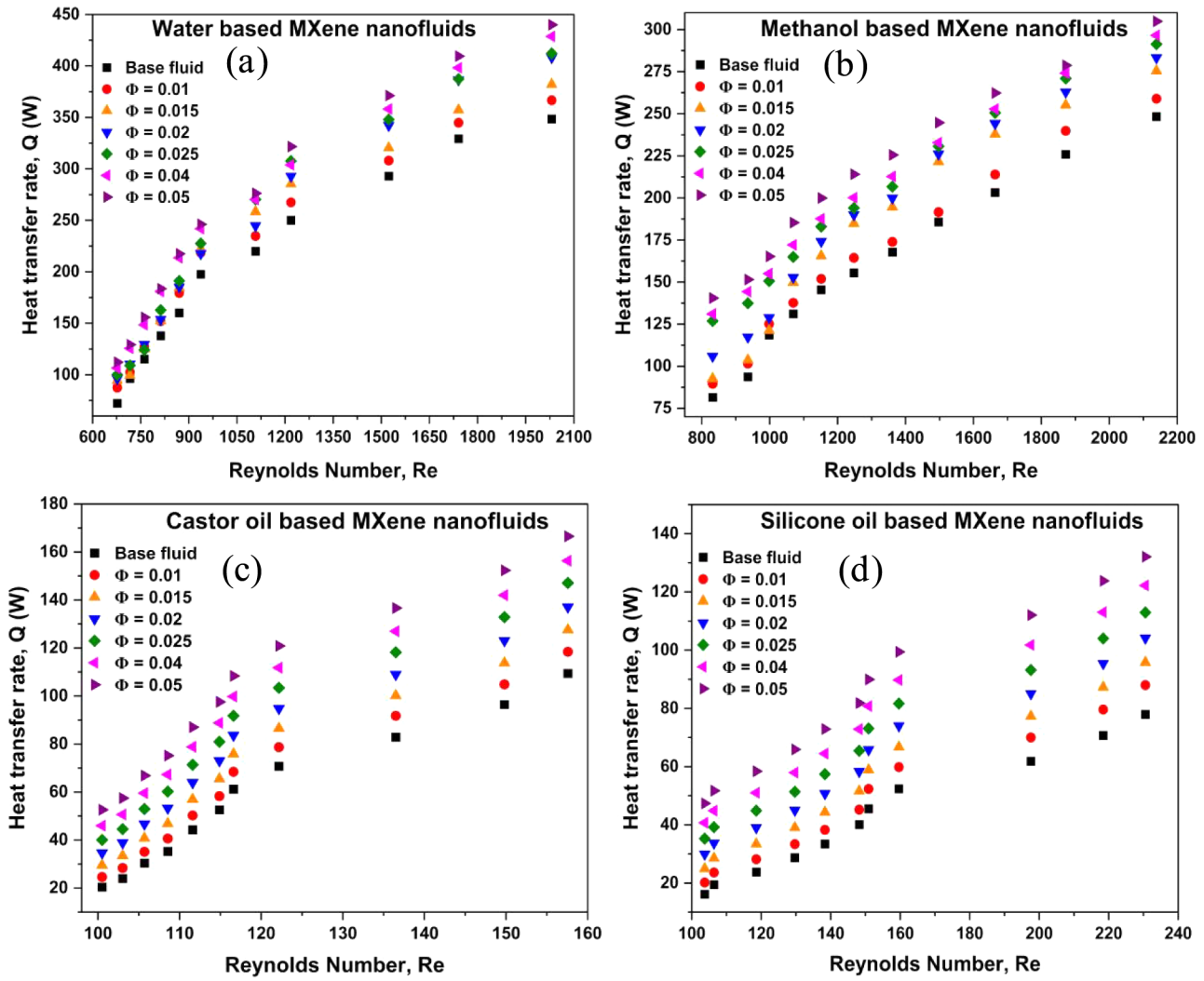

Figure 5. Effect of Re on the heat transfer rate of (a) water-based, (b) methanol-based, (c) castor oil-based, and (d) silicone oil-based MXene nanofluids with various concentrations.

https://doi.org/10.1021/acsomega.4c06080
ACS Omega 2024, 9, 41758−41775

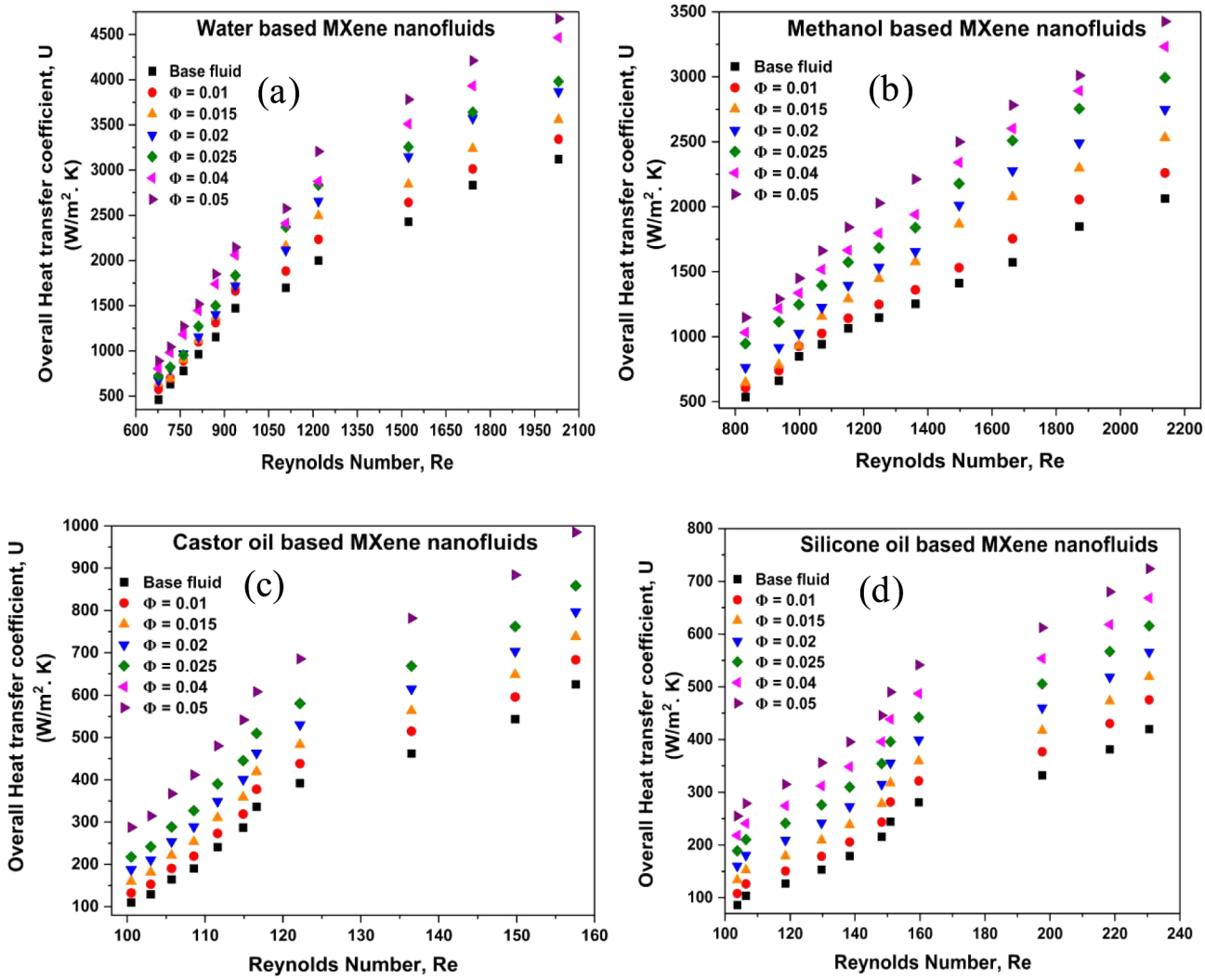

Figure 6. Effect of Re on the overall heat transfer coefficient of (a) water-based, (b) methanol-based, (c) castor oil-based, and (d) silicone oil-based MXene nanofluids at various concentrations.

Table 8. The Enhancement Percentage of *U* Compared to Their Respective Base Fluids

	% Enhancement of *U* compared to their respective base fluids			
Φ (vol %)	Water-based MXene NF	Methanol-based MXene NF	Castor oil-based MXene NF	Silicone oil-based MXene NF
0.01	12.23	9.89	13.50	16.20
0.015	19.56	23.24	28.51	33.79
0.02	26.41	34.98	44.30	52.48
0.025	33.26	53.57	60.97	72.30
0.04	48.46	64.26	78.17	92.99
0.05	59.08	78.66	97.85	118.09

3.4. Effect of Reynolds Number and Concentration of MXene Nanoparticles on the Nusselt Number. Figure 7 illustrates the effect of Reynolds number and the concentration of MXene nanoparticles on the Nusselt number for water-based, methanol-based, castor oil-based, and silicone oil-based MXene nanofluids. The Nusselt numbers for all the nanofluids were calculated using eqs 9a and 9b. Figure 7a–d shows that the Nusselt number increases with an increase in Reynolds number and concentration of nanoparticles, consistent with previous literature.[23,17,45,49] Maximum enhancements are achieved around 51.31%, 50.55%, 13.65%, and 29.82%, respectively, at a nanoparticle volume concentration of 0.05 for water-based, methanol-based, castor oil-based, and silicone oil-based nanofluids. This enhancement in Nusselt number is due to the enhancement of thermal conductivity and other thermophysical properties of the nanofluids with respect to the concentration of nanoparticles.

3.4.1. Validation of Nusselt Number. Convective heat transfer experiments were performed using the synthesized MXene nanofluids under laminar flow conditions (<2300), and the outcomes in terms of the Nusselt number revealed an acceptable level of agreement with the Nusselt number obtained from the Shah correlation shown in eq 19,[23,50,51] at low volumetric concentrations of nanoparticles compared to the Hausen correlation[50] shown in eq 20. Figure 8 shows the validation of the experimental Nusselt number with the Shah and Hausen correlation for all types of MXene nanofluids, and Tables 9 and 10 represent the analysis of R^2 values of the experimental Nusselt number with the theoretical Nusselt number P_r.

https://doi.org/10.1021/acsomega.4c06080
ACS Omega 2024, 9, 41758−41775

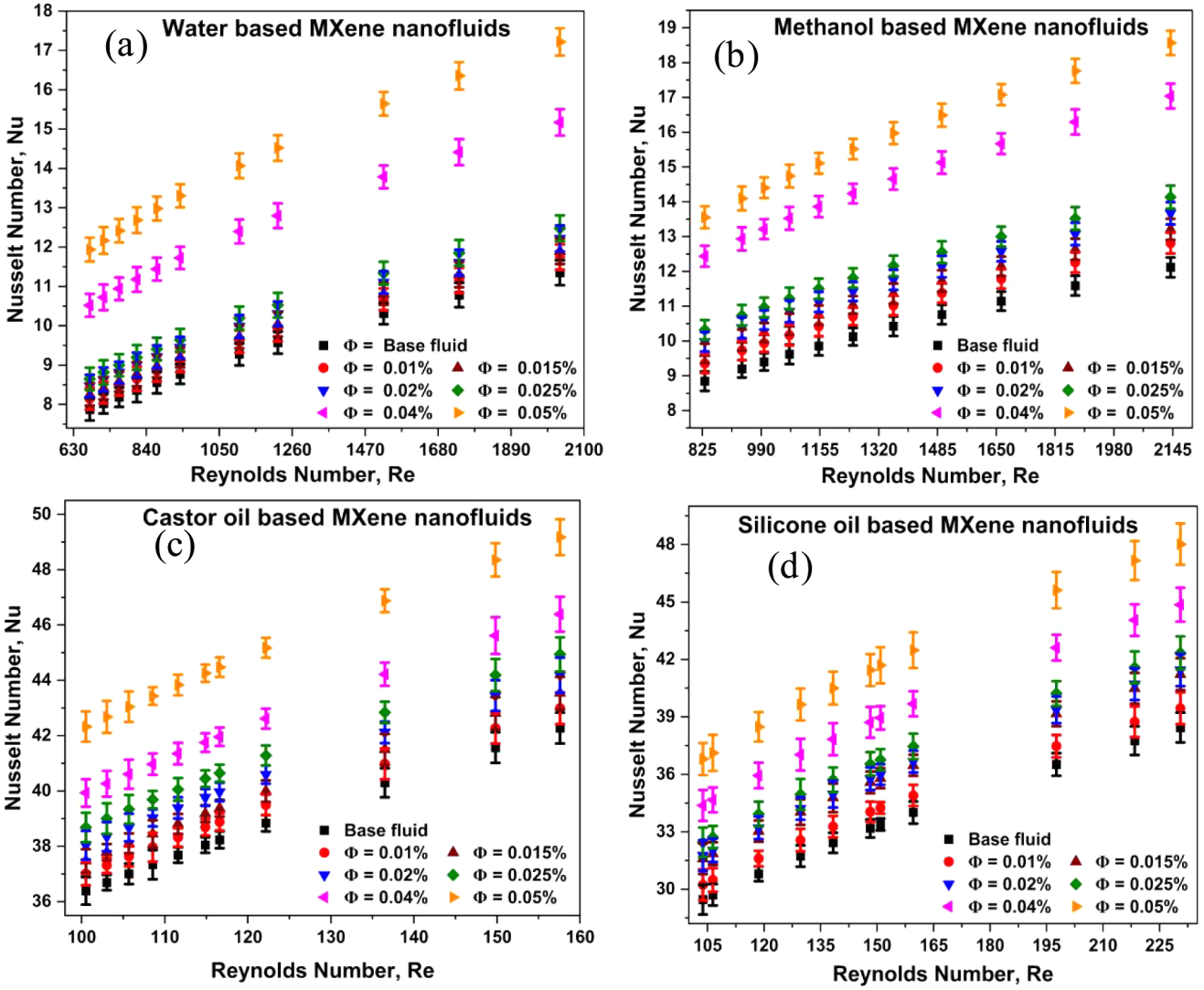

Figure 7. Effect of *Re* on Nusselt number for (a) water-based, (b) methanol-based, (c) castor oil-based, and (d) silicone oil-based MXene nanofluids at various concentrations.

$$\text{If } Pr_{nf} \times \left(\frac{D_o}{L}\right) \times Re_{nf} \geq 33.33, \quad \text{then}$$

$$N_{unf} = 1.953 \times \left((Pr_{nf} \times (\frac{D_o}{L}) \times Re_{nf})^{0.3333}\right) \tag{19}$$

$$\text{If } 0.1 < Pr_{nf} \times \left(\frac{d_e}{L}\right) \times Re_{nf} < 10^4, \quad \text{then}$$

$$N_{unf} = 3.66 + \left(\frac{\left(0.19 \times (Pr_{nf} \times (\frac{D_o}{L}) \times Re_{nf})^{0.8}\right)}{\left(1 + 0.117 \times (Pr_{nf} \times (\frac{D_o}{L}) \times Re_{nf})^{0.467}\right)}\right) \tag{20}$$

where Nu_{nf} represents nanofluid Nusselt number, Pr_{nf} shows nanofluid Prandl number, Re_{nf} signifies nanofluid Reynolds number, D_o designates outer pipe diameter, and L represents length of heat exchanger.

3.5. Effect of Reynolds Number and Concentration of MXene Nanoparticles on the Heat Transfer Coefficient (HTC). The increased volume concentration of the nanoparticles induces a significant increase in their viscosity, density, and thermal conductivity, followed by a decrease in the heat capacity of resulting nanofluids.[5,52] The heat transfer coefficient (h) is calculated using eq 13. HTC obtained shows considerable improvement in all four types of MXene-based nanofluids with respect to the increase in the concentration of nanoparticles compared to individual base fluids HTC.[16,17,23,45]

Figure 9 illustrates the effect of the Reynolds number and concentration of the nanoparticles on the heat transfer coefficient for various types of MXene nanofluids. From Figure 9a–d, it can be seen that the HTC increases with an increase in the Reynolds number and concentration of nanoparticles, possibly due to the enhanced thermophysical properties of nanofluids that accelerate the transfer of heat and thereby enhance the heat transfer coefficient (h).[6] The improvement of HTC in water based MXene nanofluids was found to be 75.1%; correspondingly, the enhancements in silicone oil-based, castor oil-based, and methanol-based are 42.71%, 50.25%, and 126.57%, respectively, at 0.05 vol %. Increased concentration of nanoparticles in the base fluid also results in an increase in the thermal conductivity of the nanofluid, which accelerates the flow of energy between the

https://doi.org/10.1021/acsomega.4c06080
ACS Omega 2024, 9, 41758−41775

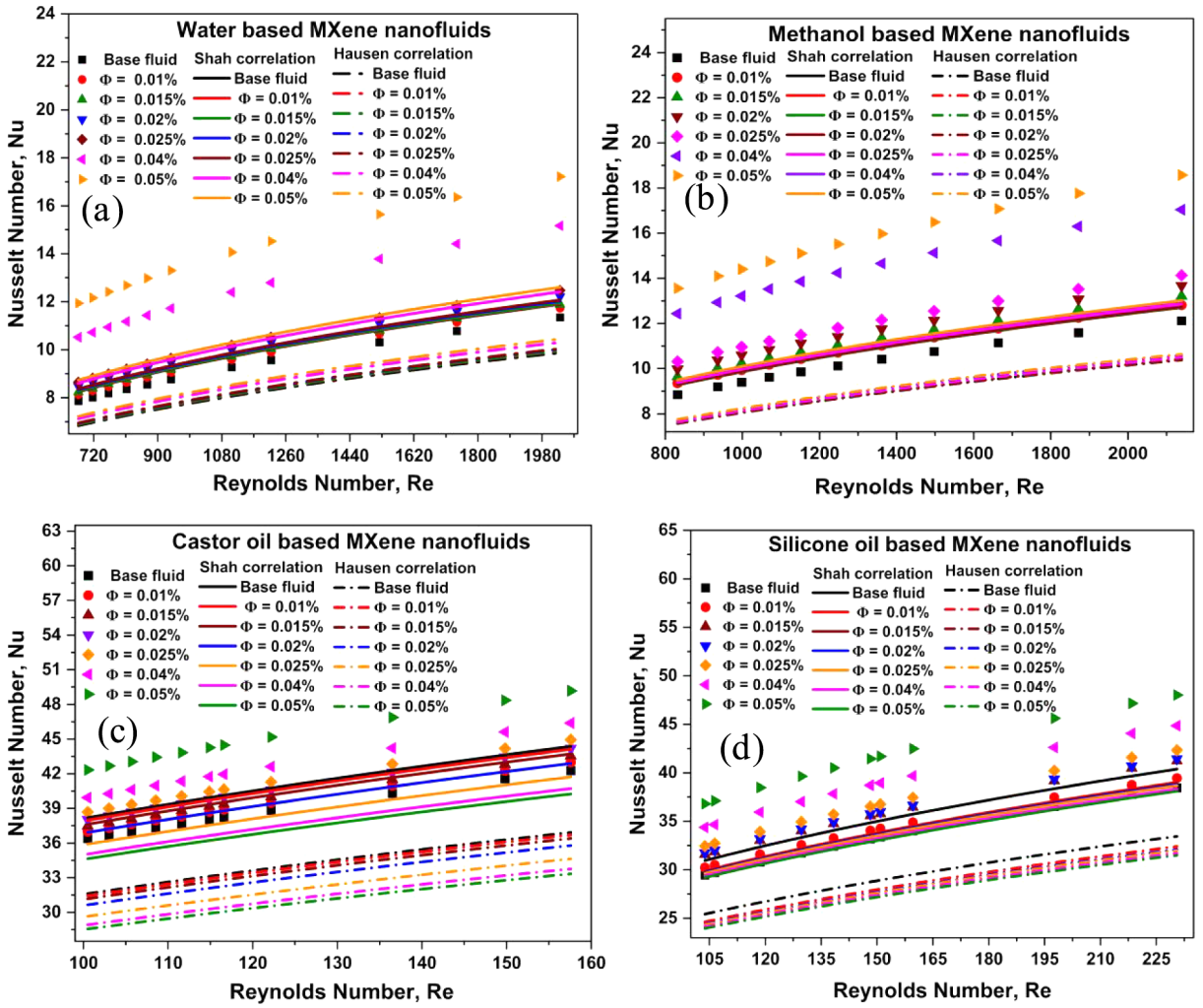

Figure 8. Validation of experimental Nusselt number correlations for (a) water-based, (b) methanol-based, (c) castor oil-based, and (d) silicone oil-based MXene nanofluids.

Table 9. R^2 Values as Per the Shah Correlation Fitment with Respect to Concentration of Nanoparticles for Different MXene Nanofluids

	R^2 Values			
Φ (vol %)	Water-based MXene NF	Methanol-based MXene NF	Castor oil-based MXene NF	Silicone oil-based MXene NF
0.0	0.99268	0.96431	0.95698	0.95178
0.01	0.98691	0.96035	0.95618	0.95142
0.015	0.98882	0.96431	0.95671	0.96548
0.02	0.99316	0.96354	0.96082	0.97651
0.025	0.98882	0.96673	0.97546	0.96221
0.04	0.98882	0.96861	0.95698	0.951369
0.05	0.98882	0.96727	0.95698	0.95562

Table 10. R^2 Values as Per the Hausen Correlation Fitment with Respect to Concentration of Nanoparticles for Different MXene nanofluids

	R^2 Values			
Φ (vol %)	Water-based MXene NF	Methanol-based MXene NF	Castor oil-based MXene NF	Silicone oil-based MXene NF
0.0	0.98589	0.95682	0.95699	0.95183
0.01	0.98639	0.95684	0.95624	0.95184
0.015	0.98943	0.96116	0.95672	0.9569
0.02	0.98606	0.95688	0.96082	0.96147
0.025	0.98213	0.9569	0.97546	0.9584
0.04	0.97912	0.95704	0.95699	0.95147
0.05	0.98236	0.95707	0.95699	0.95109

nanofluid and the heat exchanger wall and thereby improves the HTC,[5,49,53] Further, stronger intermolecular collisions caused by higher nanoparticle concentrations enhance flow dispersion and mixing, which in turn improves HTC. Enhancing the heat transfer coefficient in a convective flow is primarily accomplished by thermomigration, internal thermal conductivity of nanoparticles, and Brownian movement.[49,52]

3.6. Effect of the Reynolds Number and Concentration of Nanoparticles on the Friction Factor. Determining the friction factor of nanofluids is crucial for their prospective practical and commercial applications, in addition to their heat transfer performance.[52] The effects of the Reynolds number and concentration of nanoparticles on the friction factor are shown in Figure 10. From Figure 10a–d, it can be detected that the friction factors of all MXene nanofluids were greater than that of their respective base

https://doi.org/10.1021/acsomega.4c06080
ACS Omega 2024, 9, 41758−41775

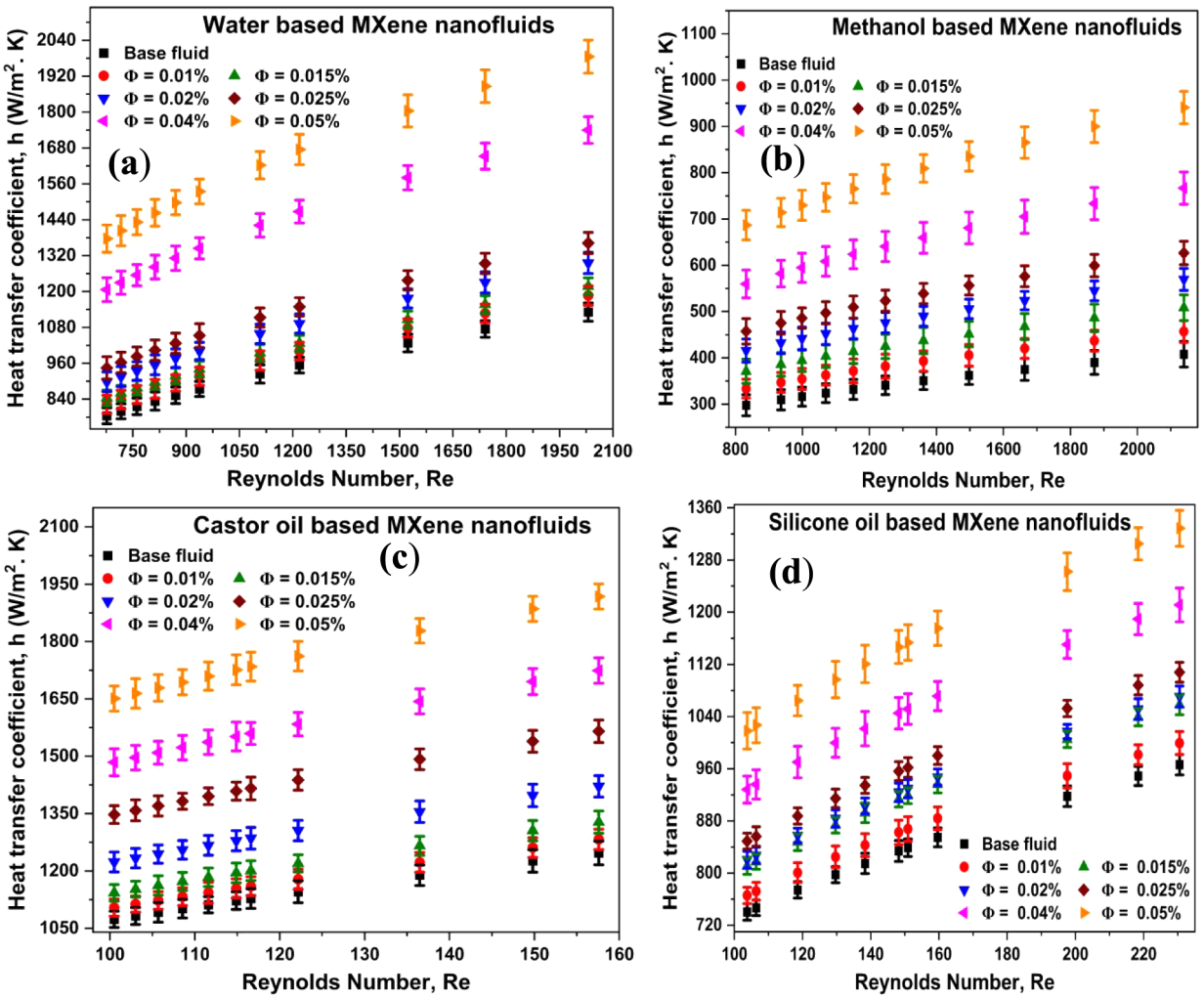

Figure 9. Effect of *Re* on the heat transfer coefficient for (a) water-based, (b) methanol-based, (c) castor oil-based, and (d) silicone oil-based MXene nanofluids at various concentrations.

fluids, which may be due to the increase in thermophysical properties and a notable contribution from the Brownian motion of the nanofluids.[6,23] In addition, the friction factor increases with respect to the increase in the concentration of nanoparticles, which could be due to additional shear stress and high viscosity exerted on the pipe wall due to maximum loading of nanoparticles.[6] The percent enhancement in friction factor of the MXene nanofluids synthesized using water, methanol, castor oil, and silicone oil as base fluids appeared to be 62%, 96%, 19%, and 34%, respectively, at high particle loading (0.05 vol %). Hence, the utilization of these nanofluids at this high concentrations of nanoparticles as cooling medium under laminar flow conditions leads to additional costs.[52]

3.7. Effect of the Reynolds Number and Concentration of the Nanoparticles on the Pressure Drop. Figure 11 shows the effect of the Reynolds number and concentration of nanoparticles on the pressure drop. From Figure 11a−d, it can be noted that the pressure drop increases with respect to the increase in the Reynolds number and concentration of nanoparticles in all the MXene nanofluids. Also, the pressure drop of the MXene-based nanofluids was greater than that of the base fluids. This kind of behavior is attributed due to the increased flow resistance caused by the higher viscosity of nanofluids at higher concentrations of nanoparticles compared to base fluids.[5,13,47,49,52,54] These MXene nanofluids indicated pressure drop enhancement of 61%, 98%, 20%, and 36%, for water-based, methanol-based, castor oil-based, and silicone oil-based nanofluids, respectively, at higher Reynolds number and volume concentrations, as represented in Figure 11a−11d.

3.8. Effect of the Reynolds Number and Concentration of Nanoparticles on the Performance Evaluation Coefficient (PEC). The performance evaluation coefficient (PEC) is a key indicator for evaluating heat exchanger performance in industries,[16,45,47] This is also referred to as the thermal performance factor (TPF)[11,12,52−56] or thermohydraulic performance.[21] PEC demonstrates the effectiveness of heat exchanger by improving the convective heat transfer and its value should be greater than unity in order to show better performance.[55] The heat exchanger performance of MXene nanofluids was estimated using eq 16. Figure 12, reveals that the PEC values are more than 1 for almost all of the MXene nanofluids. From Figure 12a,b, water-based, and methanol-based nanofluids exhibited significant performance over the whole range of volume concentration and Reynolds number. In contrast, PEC of the silicone oil-based MXene nanofluid at 0.015 vol % concentration and Reynolds number varying from 129 to 150 was less than unity (Figure 12d). Moreover, the PEC of castor oil-based MXene nanofluids with concentrations ranging from 0.01−0.025 vol % and Reynolds numbers varying

https://doi.org/10.1021/acsomega.4c06080
ACS Omega 2024, 9, 41758−41775

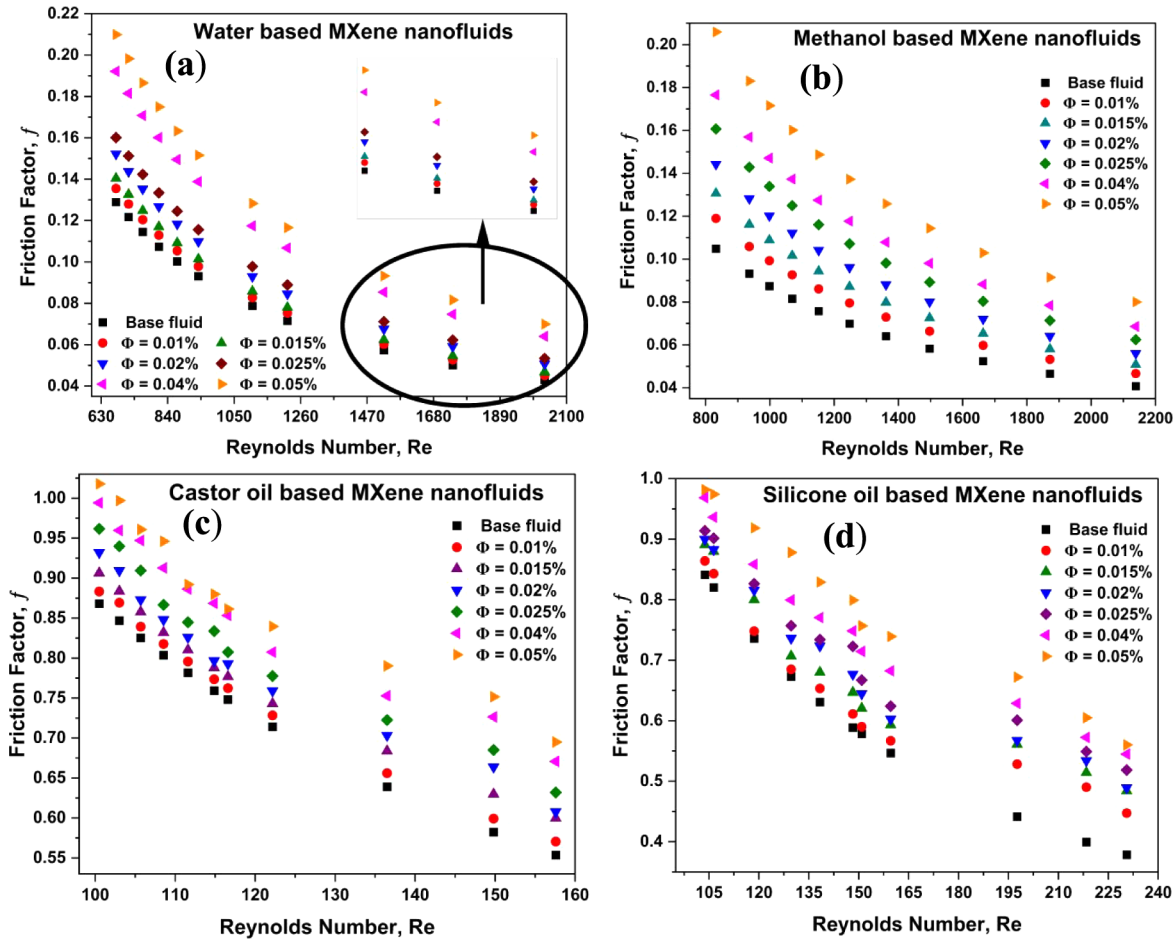

Figure 10. Effect of *Re* on the friction factor for (a) water-based, (b) methanol-based, (c) castor oil-based, and (d) silicone oil-based MXene nanofluids at various concentrations.

from 136 to 157 also exhibited less than unity (Figure 12c). Thus, it is reasonable to say that methanol- and water-based MXene nanofluids function more effectively than silicone and castor oil-based MXene nanofluids.

3.9. Comparison of Heat Transfer Parameters with Previous Studies. A comparison of the findings from the current research work with those from previous studies is displayed in Table 8. From Table 11, it can be seen that the MXene nanofluids used in the current work hold superior enhancement in heat transfer capabilities compared to other nanomaterial-based nanofluids, possibly due to the excellent stability and thermal conductivity of MXene nanostructures.

3.10. Mechanism of Heat Transfer and Flow Behavior. MXene-based nanofluids were circulated on the shell side of the double-pipe heat exchanger to study the convective heat transfer performance of the double pipe heat exchanger. From the experimental results, it was observed that the heat transfer parameters, such as the Nusselt number (Nu), overall heat transfer coefficient (U), convective heat transfer coefficient, and rate of heat transfer (Q), increased immensely with respect to the concentration of MXene nanoparticles and Reynolds number. The main mechanism behind the increase in the heat transfer parameters is due to the dispersion of MXene nanoparticles in base fluids. MXene nanoparticle dispersion in base fluids increases the thermal conductivity of base fluids; as a result, a high energy exchange process occurred due to the movement of MXene nanoparticles, which leads to enhancement in convective heat transfer. The large increase in thermal conductivity may also be due to the large surface area resulting from the layered structure of the MXene nanoparticles. This peculiar nature of MXene helps in increasing the thermal conductivity of base fluids even at a low concentrations of MXene nanoparticles.

The flow behavior of MXene nanofluids was analyzed by estimating the pressure drop and friction factor. It was observed that the pressure drop increased for all MXene nanofluids with increasing the particle concentration. As the particle concentration increased, the viscosity of the solution increased, and as a result the pressure drop is also increased. However, a slight increase in the friction factor noticed due to an increase in the concentration of MXene nanoparticles, which was similar to other works conducted by several researchers in the literature. Since, we have dispersed very low concentrations of MXene nanoparticles (less than 0.05 vol %), the increase in the friction factor was minimum. The domination of high thermal conductivity due to the layered 2D MXene nanoparticles over the increase in friction factor resulted in the enhancement of the performance of DPHE. Hence, we did not provide any external power to achieve enhancement in the performance of DPHE. Moreover, the friction factor of MXene nanofluids was greater than all the base fluids and also increased with the increase in the concentration of MXene nanoparticles. The possible mechanism for this enhancement could be due to additional shear

https://doi.org/10.1021/acsomega.4c06080
ACS Omega 2024, 9, 41758−41775

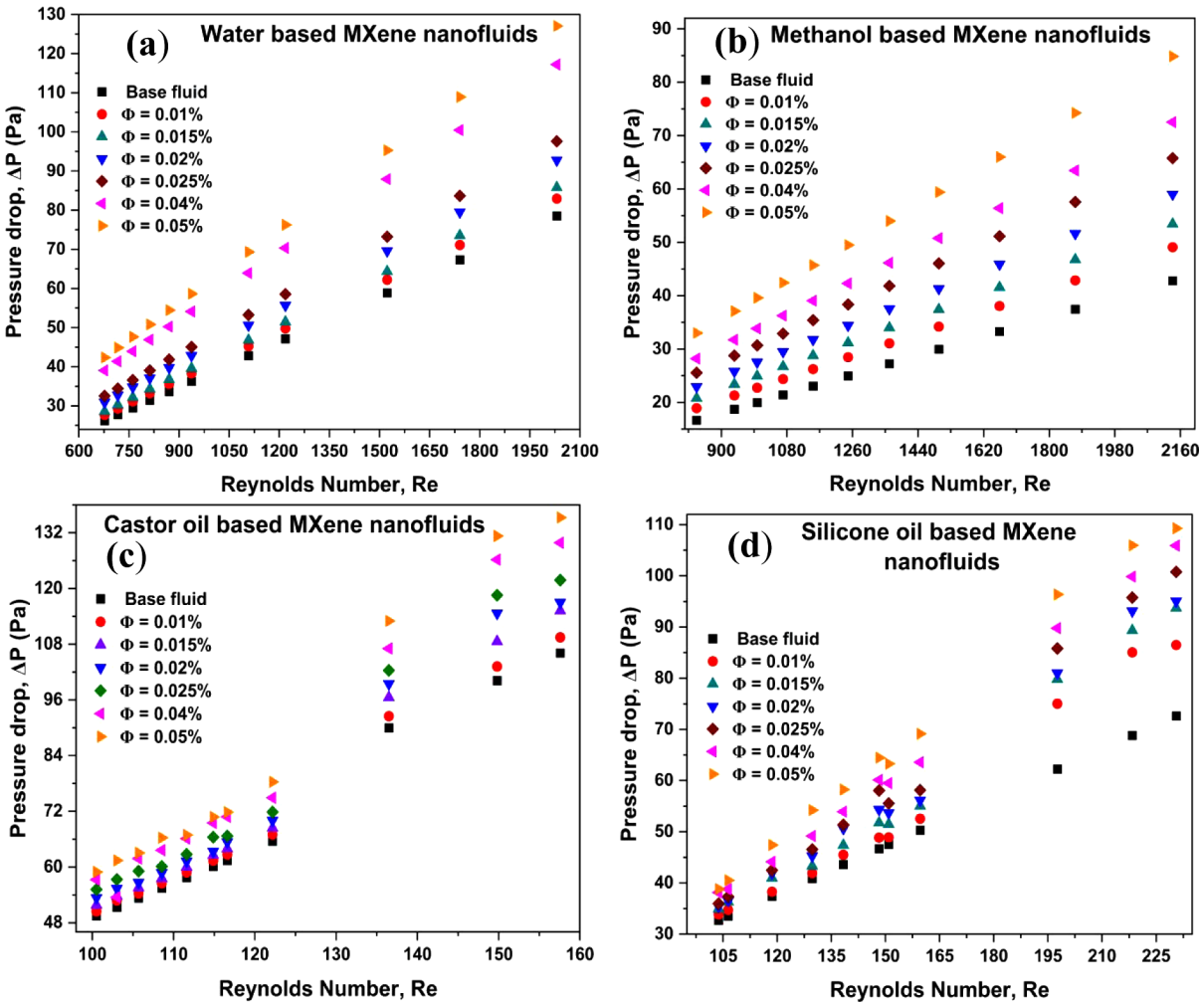

Figure 11. Effect of *Re* on the pressure drop for (a) water-based, (b) methanol-based, (c) castor oil-based, and (d) silicone oil-based MXene nanofluids at various concentrations.

stress and high viscosity that was created on the pipe wall due to the increasing concentration of nanoparticles.

3.11. Cost Analysis. Moreover, a relevant cost analysis was also conducted based on the material of construction, specifications of the DPHE, and flow parameters using the Hall method.[60]

The total cost of each heat exchanger can be calculated using the Hall technique as follows.

$$C_T = C_{OP} + C_I \tag{21}$$

where C_T, C_{OP}, and C_I represent total cost, annual operating cost, and initial investment, respectively.

The heat exchanger area influences the initial investment cost, which can be computed using the following equation.

$$C_I = (b_2 \times A^{b_3}) + b_1 \tag{22}$$

where A is the area of heat exchanger (m^2).

As the heat exchanger is fabricated from stainless steel, the b_1, b_2, and b_3 values for stainless steel are considered to be 8000, 259.2, and 0.9, respectively.[61]

The annual operating cost is determined using the below equation.:

$$C_{OP} = \sum_{K=1}^{n} \frac{C_o}{(1+i)^K} \tag{23}$$

where C_O stands for the yearly cost of operation and is given by the following equation,

$$C_o = P \times C_e \times H \tag{24}$$

$$P = \frac{1}{\eta} \times \left(\frac{\dot{m}_s}{\rho_s} \times \Delta P_s + \frac{\dot{m}_t}{\rho_t} \times \Delta P_t \right) \tag{25}$$

where subscripts s and t represent the shell side and tube side, respectively. η is the efficiency of the pump and considered as 70%.

The lifespan of the project (n), interest rate (i), and total annual operating hours (H) areassumed to be 5 years, 25%, and 2190 h/year, respectively, and utility cost (Ce) is assumed to be 0.12. The average rate of interest "i" for normal industries is 25%. The following experimental data shown in Table 12 are considered and substituted in the above equations to determine the total cost of the heat exchanger.

Finally, the initial investment cost (C_I), annual operating cost (C_{OP}), and total cost of the DPHE (C_T) is calculated using the above equations, and the values were found to be $ 8741.5, $2.86, and $ 8744, respectively.

https://doi.org/10.1021/acsomega.4c06080
ACS Omega 2024, 9, 41758−41775

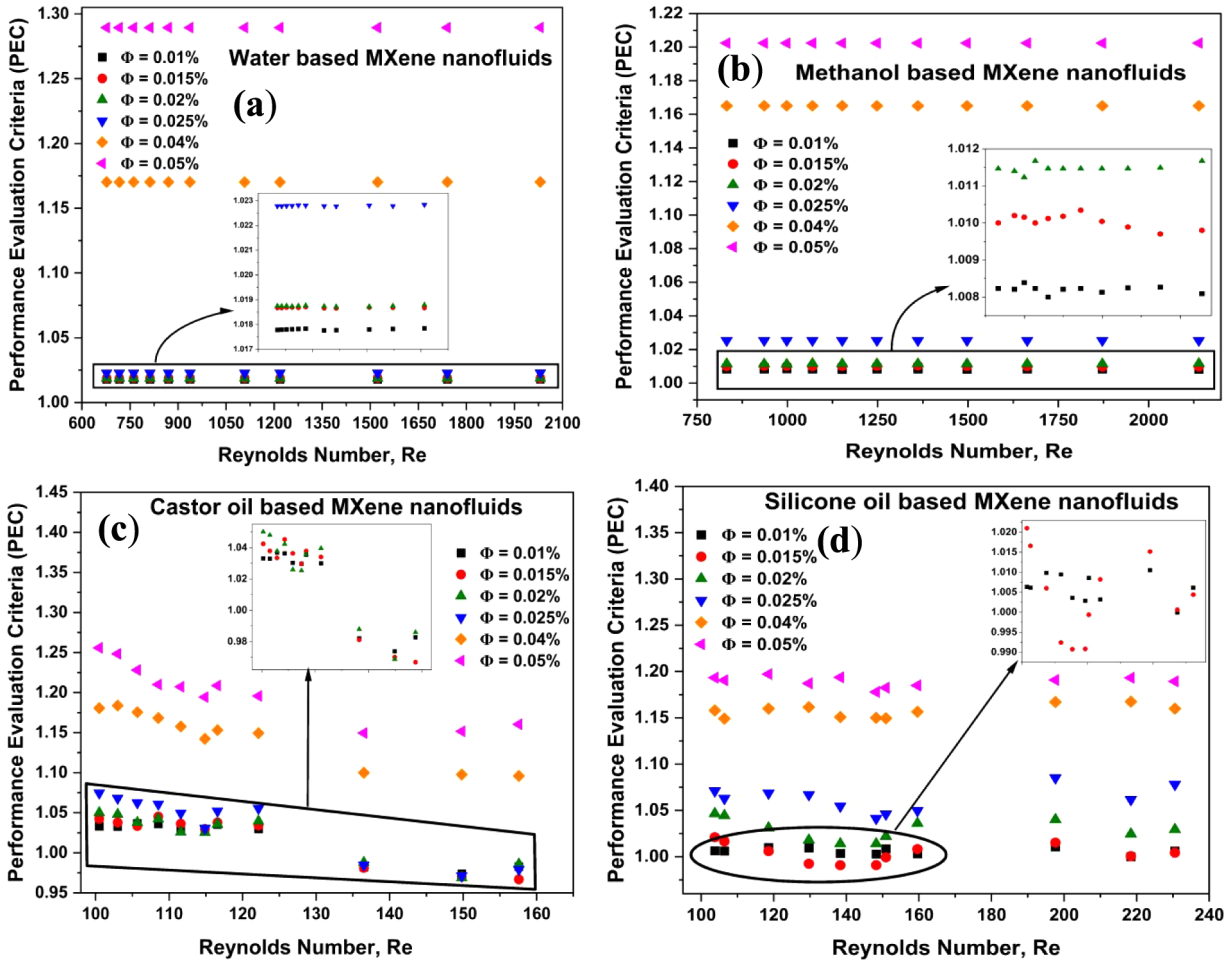

Figure 12. Effect of Re on PEC for (a) water-based, (b) methanol-based, (c) castor oil-based, and (d) silicone oil-based MXene nanofluids at various concentrations.

Table 11. The Comparison of Current work with Existing Literature

References	Nanoparticles	Concentration	Base fluid	Flow regime	Percentage enhancement (%)				PEC
					Nu	*h*	Δ*P*	*f*	
[5]	TiO_2	0.2 vol %	Water	Turbulent	-	11	12.5	12.5	-
[6]	GO	0.01−0.1 vol %	Water	Turbulent	-	85	111	72	-
[12]	SiO_2	0.5−4 vol %	Water	Turbulent	32.7	-	-	17.1	1.6
[16]	MXene	0.010.1 wt %	Ionanofluid	Laminar	136	-	-	-	1.68
[45]	MXene	0.013−0.027 vol %	DI water	Laminar	40.5	-	-	-	1.27
[57]	CuO	0.05−0.2 vol %	Water	Transition—turbulent	66	-	75	62	2.5
[58]	TiB_2	2 wt %	PG/H_2O	Turbulent	27	11	10	7	1.01
[59]	ZnO	0.5−1.25 vol %	Alkaline water	Turbulent	-	18.5	-	-	1.13
Current work	MXene	0.01 to 0.05 vol %	Water, Methanol, Castor oil, and Silicone oil	Laminar	13−51.3	42−126	19−98	20−96	1.01−1.29

Table 12. Table Representing the Fluid Properties Obtained from Experimental Data

Mass flow rate of nanofluids ($\dot{m}_s$)	0.01812 kg/s
Mass flow rate of hot water ($\dot{m}_t$)	0.00611 kg/s
Pressure drop in shell side (ΔP_s)	127.0656 Pa
Pressure drop in tube side (ΔP_t)	11.07 Pa
Density of hot water (ρ_t)	988.04 kg/m^3
Density of nanofluid (ρ_s)	997.144 kg/m^3

4. UNCERTAINTY ANALYSIS

Convective heat transfer studies of pure base fluids and MXene nanofluids were repeated three times to achieve accuracy in the results. Typically, the precision of each procedure and measurement tool affected the accuracy of the experimental data. The uncertainty of the parameters was estimated according to Kline and McClintock's implementation of the root sum square combination of the effects of each individual input and Moffat's error propagation.[10,55] Tables 13 and 14 convey an overview of the uncertainty analysis of the instruments and MXene nanofluids.

https://doi.org/10.1021/acsomega.4c06080
ACS Omega 2024, 9, 41758−41775

Table 13. Error in the Instrument

Measured parameters	Error
Temperature of inlet hot fluid	±0.2 °C
Temperature of outlet hot fluid	±0.2 °C
Temperature of inlet MXene NF	±0.2 °C
Temperature of outlet MXene NF	±0.2 °C
Speed of peristaltic pump	±1 rpm
Flow rate measured	±0.3 mL/s
Time measurement for steady state	±3 s

Table 14. The Uncertainty Analysis of MXene Nanofluids

Variables	Uncertainty in %
Reynolds number (Re)	2.46
Heat transfer rate (Q)	3.24
Nusselt number (Nu)	0.86
Heat transfer coefficient (h)	0.75
Darcy Friction factor (f)	0.55

Equations 26−30 are used in this experimental study to calculate the uncertainties of the heat transfer rate (Q_c), heat transfer coefficient (h), Reynolds number (Re), friction factor (f), and Nusselt number (Nu). Uncertainty values for density, viscosity, and thermal conductivity were already reported in our previously published work.[44]

The sample uncertainty calculations are shown below for water-based MXene nanofluid of 0.01 vol % concentration of nanoparticles.

$$u_{,Qc} = \sqrt{\left(\frac{\Delta \dot{m}_c}{\dot{m}_c}\right)^2 + \left(\frac{\Delta T}{T}\right)^2 + \left(\frac{\Delta C_{pc}}{C_{pc}}\right)^2}$$
$$= \sqrt{(0.025)^2 + (0.01)^2 + (0)^2} = 0.027\% \quad (26)$$

$$u_{,h} = \sqrt{\left(\frac{\Delta T}{T}\right)^2 + \left(\frac{\Delta Q}{Q}\right)^2 + \left(\frac{\Delta A}{A}\right)^2}$$
$$= \sqrt{(0.011)^2 + (0.008)^2 + (0)^2} = 0.013\% \quad (27)$$

$$u_{,Re} = \sqrt{\left(\frac{\Delta D_h}{D_h}\right)^2 + \left(\frac{\Delta \mu}{\mu}\right)^2 + \left(\frac{\Delta \rho}{\rho}\right)^2 + \left(\frac{\Delta v}{v}\right)^2}$$
$$= \sqrt{(0)^2 + (0.0562)^2 + (0.00011)^2 + (0.0077)^2}$$
$$= 0.056\% \quad (28)$$

$$u_{,f} = \sqrt{\left(\frac{\Delta D_h}{D_h}\right)^2 + \left(\frac{\Delta L}{L}\right)^2 + \left(\frac{\Delta \rho}{\rho}\right)^2 + \left(\frac{\Delta v}{v}\right)^2 + \left(\frac{\Delta P}{P}\right)^2}$$
$$= \sqrt{(0)^2 + (0)^2 + (0.00011)^2 + (0.0077)^2 + (0.00166)^2}$$
$$= 0.0079\% \quad (29)$$

$$u_{,Nu} = \sqrt{\left(\frac{\Delta D_h}{D_h}\right)^2 + \left(\frac{\Delta k}{k}\right)^2 + \left(\frac{\Delta h}{h}\right)^2}$$
$$= \sqrt{(0)^2 + (0.005)^2 + (0.008)^2} = 0.0094\% \quad (30)$$

5. CONCLUSION

The convective heat transfer performance of DPHE was successfully enhanced without using any inserts. Analytical techniques were effectively utilized to assess the performance of MXene-based nanofluids in a double-pipe heat exchanger using low nanoparticle concentrations ranging from 0.01−0.05 vol % in countercurrent flow arrangement. Various convective heat transfer parameters, such as the log mean temperature difference (LMTD), overall heat transfer coefficient (U), heat transfer coefficient (h), Nusselt number (Nu), friction factor (f), pressure drop (ΔP), and performance evaluation coefficient (PEC), were determined through experimental approaches to enhance the performance of DPHE. In addition, LMTD and the overall heat transfer coefficient (U) were magnificently simulated and validated using Aspen HYSYS software for all MXene nanofluids. The maximum enhancement of Nu (∼50%) and h (∼126%) were reported for MXene nanofluids prepared using 0.05 vol % MXene nanoparticles. On the other hand, the friction factor decreases as the pressure drop increases with respect to increase in the Reynolds number for all nanofluids. Finally, the performance evaluation coefficient (PEC) also successfully represented a value greater than unity for all concentrations of water- and methanol-based MXene nanofluids, ranging from 1.01 to 1.29, suggesting the better performance of heat transfer in DPHE.

■ ASSOCIATED CONTENT

Supporting Information

The Supporting Information is available free of charge at https://pubs.acs.org/doi/10.1021/acsomega.4c06080.

DPHE ASPEN HYSYS simulation screenshot. Validation of logarithmic mean temperature difference (LMTD) and the overall heat transfer coefficient (U) using ASPEN HYSYS (PDF)

■ AUTHOR INFORMATION

Corresponding Author

Aabid Hussain Shaik − *Colloids and Polymers Research Group School of Chemical Engineering, Vellore Institute of Technology, Vellore 632014, India;* orcid.org/0000-0001-8692-3639; Email: aabidhussain.s@vit.ac.in

Author

Kodi Rajesh Kumar − *Colloids and Polymers Research Group School of Chemical Engineering, Vellore Institute of Technology, Vellore 632014, India*

Complete contact information is available at: https://pubs.acs.org/10.1021/acsomega.4c06080

Notes

The authors declare no competing financial interest.

■ ACKNOWLEDGMENTS

Authors would like to thank Vellore Institute of Technology, Vellore for providing necessary research facilities for conducting this work.

■ NOMENCLATURE

d_h, Hydraulic diameter (m); ID, inner diameter (m); OD, outer diameter (m); D_i, inner pipe diameter (m); D_{io}, inner pipe outer diameter (m); D_o, outer pipe inner diameter (m); D_{oo}, outer pipe outer diameter (m); DPHE, double pipe heat

https://doi.org/10.1021/acsomega.4c06080
ACS Omega 2024, 9, 41758−41775

exchanger; $\dot{m}$, mass flow rate (kg/s); A, cross-sectional area (m^2); c_p, specific heat (J/kg K); HTC (or) h, convective heat transfer coefficient (W/m^2 K); U, overall heat transfer coefficient (W/m^2 K); L, length of heat exchanger (m); N_u, Nusselt number $\left(\frac{h^* d}{k}\right)$; P_r, Prandtl number $\left(\frac{C_p^* \mu}{k}\right)$; R_e, Reynolds number $\left(\frac{D^* \rho^* v}{\mu}\right)$; T, temperature (°C); t, time (s); v, fluid velocity (m/s); k, thermal conductivity (W/m. K); MX, MXene; TiC, titanium carbide; EG, ethylene glycol; SDS, sodium dodecyl sulfate; RPM, revolutions per minute; PID, proportional integral derivative; wt, weight (gm); P, wetted perimeter; Q, heat transfer rate (W); CFD, computational fluid dynamics; PEC, performance evaluation coefficient; w, DPHE at wall conditions; u, uncertainty (%); vol %, volume concentration (%); NRTL, Non-Random Two-Liquid model

GREEK SYMBOLS

ΔP, pressure drop (P_a); ΔT, temperature difference (°C); μ, dynamic viscosity ($P_a s$); Φ, volume concentration; f, friction factor (−); ρ, density (kg/m^3); ε, effectiveness

SUBSCRIPTS

b, bulk; f, fluid; i, inner; o, outlet; np, nanoparticles; bf, base fluids; nf, nanofluids; cf, cold fluid; hf, hot fluid; avg, Average; LMTD, log mean temperature difference

REFERENCES

(1) Dong, J.; Zheng, Q.; Xiong, C.; Sun, E.; Chen, J. Experimental investigation and application of stability and thermal characteristics of SiO_2-ethylene-glycol/water nanofluids. *Int. J. Therm. Sci.* **2022**, *176*, 107533.

(2) Elsaid, K.; Olabi, A. G.; Wilberforce, T.; Abdelkareem, M. A.; Sayed, E. T. Environmental impacts of nanofluids: A review. *Sci. Total Environ.* **2021**, *763*, 144202.

(3) Hasan, M. F.; Danışmaz, M.; Majel, B. M. Thermal performance investigation of double pipe heat exchanger embedded with extended surfaces using nanofluid technique as enhancement. *Case Stud. Therm. Eng.* **2023**, *43*, 102774.

(4) Armstrong, M.; Sivasubramanian, M.; Selvapalam, N. Experimental investigation on the heat transfer performance analysis in silver nano-coated double pipe heat exchanger using displacement reaction. *Mater. Today: Proc.* **2021**, *45*, 2482−2490.

(5) Duangthongsuk, W.; Wongwises, S. Heat transfer enhancement and pressure drop characteristics of TiO_2-water nanofluid in a double-tube counter flow heat exchanger. *Int. J. Heat Mass Transfer* **2009**, *52*, 2059−2067.

(6) Zakeri, F.; Emami, M. R. S. Experimental and numerical investigation of heat transfer and flow of water-based graphene oxide nanofluid in a double pipe heat exchanger using different artificial neural network models. *Int. Commun. Heat Mass Transfer* **2023**, *148*, 107002.

(7) Tavousi, E.; Perera, N.; Flynn, D.; Hasan, R. Heat transfer and fluid flow characteristics of the passive method in double tube heat exchangers: A critical review. *Int. J. Thermofluids* **2023**, *17*, 100282.

(8) Al-Obaidi, A. R.; Chaer, I. Study of the flow characteristics, pressure drop and augmentation of heat performance in a horizontal pipe with and without twisted tape inserts. *Therm. Eng.* **2021**, *25*, 100964.

(9) Sahiti, N.; Durst, F.; Dewan, A. Heat transfer enhancement by pin elements. *Int. J. Heat Mass Transfer* **2005**, *48*, 4738−4747.

(10) Salem, M. R.; Althafeeri, M. K.; Elshazly, K. M.; Higazy, M. G.; Abdrabbo, M. F. Experimental investigation on the thermal performance of a double pipe heat exchanger with segmental perforated baffles. *Int. J. Therm. Sci.* **2017**, *122*, 39−52.

(11) Dizaji, H. S.; Jafarmadar, S.; Mobadersani, F. Experimental studies on heat transfer and pressure drop characteristics for new arrangements of corrugated tubes in a double pipe heat exchanger. *Int. J. Therm. Sci.* **2015**, *96*, 211−220.

(12) Venkitaraj, K. P.; Suresh, S.; Alwin Mathew, T.; Bibin, B. S.; Abraham, J. An experimental investigation on heat transfer enhancement in the laminar flow of water/TiO_2 nanofluid through a tube heat exchanger fitted with modified butterfly inserts. *Heat Mass Transfer* **2018**, *54*, 813−829.

(13) Azmi, W. H.; Sharma, K. V.; Sarma, P. K.; Mamat, R.; Anuar, S.; Dharma Rao, V. Experimental determination of turbulent forced convection heat transfer and friction factor with SiO_2 nanofluid. *Exp. Therm. Fluid Sci.* **2013**, *51*, 103−111.

(14) Sheikholeslami, M.; Bhatti, M. M. Active method for nanofluid heat transfer enhancement by means of EHD. *Int. J. Heat Mass Transfer* **2017**, *109*, 115−122.

(15) Ravi Kumar, N. T.; Bhramara, P.; Addis, B. M.; Sundar, L. S.; Singh, M. K.; Sousa, A. C. M. Heat transfer, friction factor and effectiveness analysis of Fe_3O_4/water nanofluid flow in a double pipe heat exchanger with return bend, Int. *Commun. Heat Mass Transfer* **2017**, *81*, 155−163.

(16) Das, L.; Rubbi, F.; Habib, K.; Saidur, R.; Islam, N.; Saha, B. B.; Aslfattahi, N.; Irshad, K. Hydrothermal performance improvement of an inserted double pipe heat exchanger with Ionanofluid. *Case Stud. Therm. Eng.* **2021**, *28*, 101533.

(17) Ravi Kumar, N. T.; Bhramara, P.; Sundar, L. S.; Singh, M. K.; Sousa, A. C. M. Heat transfer, friction factor and effectiveness of Fe_3O_4 nanofluid flow in an inner tube of double pipe U-bend heat exchanger with and without longitudinal strip inserts. *Exp. Therm. Fluid Sci.* **2017**, *85*, 331−343.

(18) Tiwari, A. K.; Javed, S.; Oztop, H. F.; Said, Z.; Pandya, N. S. Experimental and numerical investigation on the thermal performance of triple tube heat exchanger equipped with different inserts with WO_3/water nanofluid under turbulent condition. *Int. J. Therm. Sci.* **2021**, *164*, 106861.

(19) Khedkar, R. S.; Sonawane, S. S.; Wasewar, K. L. Heat transfer study on concentric tube heat exchanger using TiO_2-water based nanofluid. *Int. Commun. Heat Mass Transfer* **2014**, *57*, 163−169.

(20) Darzi, A. A. R.; Farhadi, M.; Sedighi, K. Heat transfer and flow characteristics of Al_2O_3-water nanofluid in a double tube heat exchanger. *Int. Commun. Heat Mass Transfer* **2013**, *47*, 105−112.

(21) Mukherjee, S.; Wciślik, S.; Mishra, P. C.; Chaudhuri, P. Nanofluids: Critical issues, economics and sustainability perspectives. *Particuology* **2024**, *87*, 147−172.

(22) Choi, S. U. S.; Eastman, J. A. Enhancing thermal conductivity of fluids with nanoparticles. *1995 International mechanical engineering congress and exhibition* **1995**, 99−105.

(23) Suresh, S.; Venkitaraj, K. P.; Selvakumar, P.; Chandrasekar, M. Effect of Al_2O_3-Cu/water hybrid nanofluid in heat transfer. *Exp. Therm. Fluid Sci.* **2012**, *38*, 54−60.

(24) Jayranaiwachira, N.; Promvonge, P.; Thianpong, C.; Skullong, S. Entropy generation and thermal performance of tubular heat exchanger fitted with louvered corner-curved V-baffles. *Int. J. Heat Mass Transfer* **2023**, *201*, 123638.

(25) Wu, X.; Fu, T.; Wang, J.; Zeng, L.; Zhang, F. A comparative study of fluid flow and heat transfer in the tube with multi-V-winglets vortex generators. *Appl. Therm. Eng.* **2024**, *236*, 121448.

(26) Louahdi, M.; Salhi, J. E.; Essaouini, H.; Zarrouk, T.; Lahlaouti, M. L. Three-Dimensional Analysis for Optimizing Thermo-Hydrodynamic Performance of Heat Exchangers with Perforated Semi-Circular Inserts. *Case Stud. Therm. Eng.* **2024**, *60*, 104611.

(27) Kavitha, R.; Methkal Abd Algani, Y.; Kulkarni, K.; Gupta, M. K. Heat transfer enhancement in a double pipe heat exchanger with copper oxide nanofluid: An experimental study. *Mater. Today: Proc.* **2022**, *56*, 3446−3449.

(28) Sajid, M. U.; Ali, H. M. Recent advances in application of nanofluids in heat transfer devices: A critical review. *Renewable Sustainable Energy Rev.* **2019**, *103*, 556−592.

https://doi.org/10.1021/acsomega.4c06080
ACS Omega 2024, 9, 41758−41775

(29) Naguib, M.; Kurtoglu, M.; Presser, V.; Lu, J.; Niu, J.; Heon, M.; Hultman, L.; Gogotsi, Y.; Barsoum, M. W. Two-dimensional nanocrystals produced by exfoliation of Ti_3AlC_2. *Adv. Mater.* **2011**, *23*, 4248−4253.
(30) Gogotsi, Y.; Anasori, B. The Rise of MXenes. *ACS Nano* **2019**, *13*, 8491−8494.
(31) Ma, X.; Yang, L.; Xu, G.; Song, J. A comprehensive review of MXene-based nanofluids: Preparation, stability, physical properties, and applications. *J. Mol. Liq.* **2022**, *365*, 120037.
(32) Salim, O.; Mahmoud, K. A.; Pant, K. K.; Joshi, R. K. Introduction to MXenes: synthesis and characteristics. *Mater. Today Chem.* **2019**, *14*, 100191.
(33) Kumar, E. A.; Kokulnathan, T.; Wang, T. J.; Anthuvan, A. J.; Chang, Y. H. Two-dimensional titanium carbide (MXene) nanosheets as an efficient electrocatalyst for 4-nitroquinoline N-oxide detection. *J. Mol. Liq.* **2020**, *312*, 113354.
(34) Alwarappan, S.; Nesakumar, N.; Sun, D.; Hu, T. Y.; Li, C. Z. 2D metal carbides and nitrides (MXenes) for sensors and biosensors. *Biosens. Bioelectron.* **2022**, *205*, 113943.
(35) Warsi, A. Z.; Aziz, F.; Zulfiqar, S.; Haider, S.; Shakir, I.; Agboola, P. O. Synthesis, characterization, photocatalysis, and antibacterial study of WO_3, MXene and WO_3/MXene nanocomposite. *Nanomaterials* **2022**, *12*, 713.
(36) Hwang, S. K.; Kang, S. M.; Rethinasabapathy, M.; Roh, C.; Huh, Y. S. MXene: An emerging two-dimensional layered material for removal of radioactive pollutants. *Chem. Eng. J.* **2020**, *397*, 125428.
(37) Tang, M.; Li, J.; Wang, Y.; Han, W.; Xu, S.; Lu, M.; Zhang, W.; Li, H. Surface terminations of MXene: synthesis, characterization, and properties. *Symmetry* **2022**, *14*, 2232.
(38) Kumar Singh, S.; Kumar Tiwari, A.; Paliwal, H. K. A holistic review of MXenes for solar device applications: Synthesis, characterization, properties and stability. *FlatChem* **2023**, *39*, 100493.
(39) Anasori, B.; Lukatskaya, M. R.; Gogotsi, Y. 2D metal carbides and nitrides (MXenes) for energy storage. *Nat. Rev. Mater.* **2017**, *2*, 1−17.
(40) Yuen, A. C. Y.; Chen, T. B. Y.; Lin, B.; Yang, W.; Kabir, I. I.; De Cachinho Cordeiro, I. M.; Whitten, A. E.; Mata, J.; Yu, B.; Lu, H. D.; Yeoh, G.H. Study of structure morphology and layer thickness of Ti_3C_2 MXene with Small-Angle Neutron Scattering (SANS). *Compos., Part C: Open Access* **2021**, *5*, 100155.
(41) Rubbi, F.; Habib, K.; Saidur, R.; Aslfattahi, N.; Yahya, S. M.; Das, L. Performance optimization of a hybrid PV/T solar system using Soybean oil/MXene nanofluids as A new class of heat transfer fluids. *Sol. Energy* **2020**, *208*, 124−138.
(42) Aslfattahi, N.; Samylingam, L.; Abdelrazik, A. S.; Arifutzzaman, A.; Saidur, R. MXene based new class of silicone oil nanofluids for the performance improvement of concentrated photovoltaic thermal collector. *Sol. Energy Mater. Sol. Cells* **2020**, *211*, 110526.
(43) Samylingam, L.; Aslfattahi, N.; Saidur, R.; Yahya, S. M.; Afzal, A.; Arifutzzaman, A.; Tan, K. H.; Kadirgama, K. Thermal and energy performance improvement of hybrid PV/T system by using olein palm oil with MXene as a new class of heat transfer fluid. *Sol. Energy Mater. Sol. Cells* **2020**, *218*, 110754.
(44) Kumar, K. R.; Shaik, A. H. Synthesis, thermophysical characterization and thermal performance analysis of novel Cu-MXene hybrid nanofluids for efficient coolant applications. *RSC Adv.* **2023**, *13*, 29536−29560.
(45) Ambreen, T.; Saleem, A.; Park, C. W. Thermal efficiency of eco-friendly MXene based nanofluid for performance enhancement of a pin-fin heat sink: Experimental and numerical analyses. *Int. J. Heat Mass Transfer* **2022**, *186*, 122451.
(46) Garud, K. S.; Lee, M. Y. Numerical investigations on heat transfer characteristics of single particle and hybrid nanofluids in uniformly heated tube. *Symmetry* **2021**, *13*, 876.
(47) Çolak, A. B.; Açikgöz, Ö.; Mercan, H.; Dalkiliç, A. S.; Wongwises, S. Prediction of heat transfer coefficient, pressure drop, and overall cost of double-pipe heat exchangers using the artificial neural network. *Case Stud. Therm. Eng.* **2022**, *39*, 102391.
(48) Singh, S.; Verma, P.; Ghosh, S. K. Numerical and experimental analysis of performance in a compact plate heat exchanger using graphene oxide/water nanofluid. *Int. J. Numer. Methods Heat Fluid Flow* **2021**, *31*, 3356−3372.
(49) Chandrasekar, M.; Suresh, S.; Bose, A. C. Experimental studies on heat transfer and friction factor characteristics of Al_2O_3/water nanofluid in a circular pipe under laminar flow with wire coil inserts. *Exp. Therm. Fluid Sci.* **2010**, *34* (2), 122−130.
(50) Shah, R. K. Thermal entry length solutions for the circular tube and parallel plates. In *Proceedings of Third National Heat Mass Transfer Conference*, Indian Institute of Technology: Bombay, (Paper No. HMT-11−75), 1975.
(51) Syam Sundar, L. Heat transfer, friction factor and exergy efficiency analysis of nanodiamond-Fe_3O_4/water hybrid nanofluids in a tube with twisted tape inserts. *Ain Shams Eng. J.* **2023**, *14*, 102068.
(52) Sarafraz, M. M.; Hormozi, F. Intensification of forced convection heat transfer using biological nanofluid in a double-pipe heat exchanger. *Exp. Therm. Fluid Sci.* **2015**, *66*, 279−289.
(53) Ramadhan, A. I.; Azmi, W. H.; Mamat, R.; Hamid, K. A. Experimental and numerical study of heat transfer and friction factor of plain tube with hybrid nanofluids. *Case Stud. Therm. Eng.* **2020**, *22*, 100782.
(54) Goodarzi, M.; Kherbeet, A. S.; Afrand, M.; Sadeghinezhad, E.; Mehrali, M.; Zahedi, P.; Wongwises, S.; Dahari, M. Investigation of heat transfer performance and friction factor of a counter-flow double-pipe heat exchanger using nitrogen-doped, graphene-based nanofluids. *Int. Commun. Heat Mass Transfer* **2016**, *76*, 16−23.
(55) Dhumal, G. S.; Havaldar, S. N. Enhancing heat transfer performance in a double tube heat exchanger: Experimental study with twisted and helical tapes. *Case Stud. Therm. Eng.* **2023**, *51*, 103613.
(56) Poongavanam, G. K.; Kumar, B.; Duraisamy, S.; Panchabikesan, K.; Ramalingam, V. Heat transfer and pressure drop performance of solar glycol/activated carbon based nanofluids in shot peened double pipe heat exchanger. *Renewable Energy* **2019**, *140*, 580−591.
(57) Salameh, T.; Alkasrawi, M.; Olabi, A. G.; Al Makky, A.; Abdelkareem, M. A. Experimental and numerical analysis of heat transfer enhancement inside concentric counter flow tube heat exchanger using different nanofluids. *Int. J. Thermofluids* **2023**, *20*, 100432.
(58) Vallejo, J. P.; Ansia, L.; Calviño, U.; Marcos, M. A.; Fernández-Seara, J.; Lugo, L. Convection behaviour of mono and hybrid nanofluids containing B_4C and TiB_2 nanoparticles. *Int. J. Therm. Sci.* **2023**, *189*, 108268.
(59) Yogaraj, D.; Deepak, S. S. K.; Rakshgan, G. J.; Dwarakesh, P.; Vishwakarma, R.; Kujur, P. K.; Rao, Y. A. Thermal performance analysis of a counter-flow double-pipe heat exchanger using titanium oxide and zinc oxide nanofluids. *Mater. Today: Proc.* **2023**.
(60) Peters, M. S.; Timmerhaus, K. D.; West, R. E. *Plant Design and Economics for Chemical Engineers*; McGraw-Hill: New York, 1968.
(61) Caputo, A. C.; Pelagagge, M. P.; Salini, P. Heat exchanger design based on economic optimization. *Appl. Therm. Eng.* **2008**, *28*, 1151−1159.

https://doi.org/10.1021/acsomega.4c06080
ACS Omega 2024, 9, 41758−41775